Double-diffusive two-fluid flow in a slippery channel: A linear stability analysis

Sukhendu Ghosh, R. Usha, and Kirti Chandra Sahu

Citation: Physics of Fluids (1994-present) **26**, 127101 (2014); doi: 10.1063/1.4902948
View online: http://dx.doi.org/10.1063/1.4902948
View Table of Contents: http://scitation.aip.org/content/aip/journal/pof2/26/12?ver=pdfcov
Published by the AIP Publishing

PHYSICS OF FLUIDS **26**, 127101 (2014)

Double-diffusive two-fluid flow in a slippery channel: A linear stability analysis

Sukhendu Ghosh,[1] R. Usha,[1,a)] and Kirti Chandra Sahu[2]
[1]*Department of Mathematics, Indian Institute of Technology Madras, Chennai 600036, India*
[2]*Department of Chemical Engineering, Indian Institute of Technology Hyderabad, Yeddumailaram 502 205, Andhra Pradesh, India*

(Received 10 March 2014; accepted 10 November 2014; published online 8 December 2014)

The effect of velocity slip at the walls on the linear stability characteristics of two-fluid three-layer channel flow (the equivalent core-annular configuration in case of pipe) is investigated in the presence of double diffusive (DD) phenomenon. The fluids are miscible and consist of two solute species having different rates of diffusion. The fluids are assumed to be of the same density, but varying viscosity, which depends on the concentration of the solute species. It is found that the flow stabilizes when the less viscous fluid is present in the region adjacent to the slippery channel walls in the single-component (SC) system but becomes unstable at low Reynolds numbers in the presence of DD effect. As the mixed region of the fluids moves towards the channel walls, a new unstable mode (DD mode), distinct from the Tollman Schlichting (TS) mode, arises at Reynolds numbers smaller than the critical Reynolds number for the TS mode. We also found that this mode becomes more prominent when the mixed layer overlaps with the critical layer. It is shown that the slip parameter has nonmonotonic effect on the stability characteristics in this system. Through energy budget analysis, the dual role of slip is explained. The effect of slip is influenced by the location of mixed layer, the log-mobility ratio of the faster diffusing scalar, diffusivity, and the ratio of diffusion coefficients of the two species. Increasing the value of the slip parameter delays the first occurrence of the DD-mode. It is possible to achieve stabilization or destabilization by controlling the various physical parameters in the flow system. In the present study, we suggest an effective and realistic way to control three-layer miscible channel flow with viscosity stratification. © *2014 AIP Publishing LLC*. [http://dx.doi.org/10.1063/1.4902948]

I. INTRODUCTION

A linear stability analysis of pressure-driven flow of two miscible fluids having the same density and varying viscosity in a channel with velocity slip at the walls has been investigated by Ghosh *et al.*[1] This study has been motivated by its relevance in many industrial applications.[2–10] Their results provide an effective strategy of flow control in a channel with slippery walls or with walls as hydrophobic surfaces. Their results are also relevant when the walls of the channel are porous substrates, with a smaller superficial velocity in the porous medium as compared to the velocity in the fluid layer. The message from their investigation is that wall slip has significant effects on the stability of the flow and it plays a dual role of either stabilizing or destabilizing the flow in a rigid channel.[11] This has been shown to be achieved by appropriately choosing the viscosity of the fluid layer adjacent to the wall and by placing the mixed layer in appropriate location in the wall-normal direction of the slippery channel. The flow has a destabilising influence when a highly viscous fluid is located adjacent to the wall with slip. In this configuration, a new mode of instability (overlap or 'O'-mode) occurs for high mass diffusivity of the two fluids. This mode appears due to the overlap of the critical layer of dominant instability with the mixed layer of

a)Author to whom correspondence should be addressed. Email: ushar@iitm.ac.in

varying viscosity (i.e., under overlap condition). Further, the stability characteristics of this system has been observed to be different from both the limiting cases of interface dominated flows[12] and continuously stratified flows in a channel with slip.[13] In addition, when compared with a single fluid flow in a rigid/slippery channel, the two-fluid channel flow in a rigid[11]/slippery[1] channel is more stable (more unstable) with a higher viscous fluid near the wall and with the mixed layer and the critical layer well separated (overlapping each other). Their investigations[1,11] focused on single component (SC) miscible system (finite diffusivity) in which the viscosity stratification has been achieved by varying the concentration of single species in the fluids. A striking feature of the instability is that for any Reynolds number, only a band of wave numbers are unstable; the flow system is stable for shorter wavelengths and smaller wave numbers. An immediate curiosity is to analyze a flow system with two diffusing species having different diffusivities, and in which the inhomogeneities in solute concentration are accounted in terms of stratified viscosity, not in terms of density as is done in the investigations by Turner,[14] Huppert,[15] May and Kelley,[16] and Worster.[17]

The linear stability analysis of such a double-diffusive (DD) three-layer flow of two miscible fluids with viscosity stratification has been considered by Sahu and Govindarajan[18–20] in a rigid channel. Their results show the existence of an unstable DD mode in a classically stable system in the context of SC flows, i.e., when the less viscous fluid is placed in the annular region and the highly viscous fluid in the core region of the channel. The DD system is observed to exhibit stability characteristics that are fundamentally different from the SC system, in the sense that the DD instability occurs when the flow is inviscidly stable based on Rayleigh's theorem[21] or stably stratified with respect to viscosity as described by Sahu and Govindarajan.[18] Their investigation clearly demonstrates the significance of viscosity stratification in a double-diffusive two-fluid flow system and is motivated by the extensive studies (Turner,[14] Huppert,[15] and May and Kelley[16]) on the stability of miscible flows where the viscosity is constant but density is dependent on the concentration of the species. Such a configuration is fundamental to a variety of naturally occurring phenomena as well as in practical applications, such as the transport of crude oil in pipelines (Joseph *et al.*[22]). Further, the mixing in chemical processes can be better understood, if one knows to assess the influence of concentration variation of the species on the fluid properties. As a consequence, there have been several recent studies which have investigated this aspect in various systems, such as porous media,[23] chemically driven systems,[24–29] and also in food processing industries and diary plants.[30]

The instabilities which arise due to viscosity stratification in different geometries, such as in miscible channel flows and core-annular miscible flows are well documented in literature, and discussed in a recent review by Govindarajan and Sahu.[31] The articles relevant to the present study have examined flow system in a rigid channel (the linear stability analysis of SC systems;[11,22,32–36] convective and absolute instabilities in SC systems[37]). They have shown that the flow has a stabilising (destabilising) influence when the less (highly) viscous fluid occupies the near wall regions of the channel for low to moderate Schmidt numbers. The presence of mixed layer destabilizes the flow at higher Schmidt numbers, and the destabilisation is enhanced as the Schmidt number increases. Also, increasing the viscosity of the annular fluid by keeping the viscosity of the core fluid the same has a destabilising influence. Sahu *et al.*[37] showed that the above system becomes absolutely unstable for a certain range of parameters and have indicated the region of absolute and convective instabilities in the Reynolds number and viscosity ratio space. There are also several investigations[29,30,38–48] not relevant to the present study (but worth mentioning in the present context) that deals with stability characteristics of viscosity stratified flows in rigid channels/pipes, involving the displacement of one fluid by another. The interesting features and the type of instabilities displayed by these flow systems with boundaries as either rigid walls or rigid circular pipes suggest that it is worth analyzing the analogous flow systems in configurations with velocity slip at the boundaries.

Pascal[49] has demonstrated that a flow of a thin Newtonian film down a saturated porous inclined substrate can be modelled by a solid substrate with a Navier-slip boundary condition $u = l\,(\partial u/\partial y)$ under the assumption that the superficial velocity in the porous layer is much smaller than the velocity in the fluid layer. Here, the effective length $l = \kappa/\alpha$, where κ is the permeability of the porous medium and α is a dimensionless parameter that depends on the structure of the porous medium. In fact, in many situations, the solid substrate is permeable. Further, it is well known that machine polished metal surfaces have surface irregularities of the order of 0.1 μm,[50] and as the

intermolecular forces are operative to at most 0.1 μm on most of the solid surfaces, the effects of surface irregularities dominate the flow at small scales. In addition, there are a number of situations, where it is necessary to provide an explanation for velocity slip on a rough surface.[9,51,52] Also, the results on microscale flows driven by pressure gradient showed an apparent break-down of the no-slip condition when slip length is as large as micrometers.[53–56] The study of Vinogradova's[57] on pressure-driven flow in a channel exhibits results consistent with slip at the wall boundary.

The above mentioned theoretical and experimental investigations suggest that it is relevant to analyze the effects of slip on the linear stability characteristics of wall bounded shear flow with velocity slip at the walls of the channel. It is important to note that such an attempt has been carried out by Gersting,[58] Spille and Rauh,[59] Gan and Wu,[60] Lauga and Cossu,[61] Ling *et al.*,[62] and Ren and Xia[63] for Poiseuille flow of single fluid with both symmetric and asymmetric slip conditions at the walls. They have observed that the slip plays a dual role by either stabilizing or destabilizing the flow system considered in their study.

The results for a flow in a divergent slippery channel[37] with Maxwell velocity slip boundary condition at the walls reveal that velocity slip at the walls has a destabilizing influence even for smaller Knudsen numbers (Kn), where Kn is the ratio of slip length to the local half-width of the channel. It is to be noted that the Navier-Stokes equations are valid for slip length up to 0.1,[64] if the slip conditions are imposed at the walls.

The influence of velocity slip at the walls on the stability characteristics of viscosity-stratified flow in a microchannel, wherein two immiscible fluids separated by a sharp interface has been examined by You and Zheng.[12] It is shown that velocity slip at the walls enhances the stability of stratified microchannel flow. The effects of velocity slip are found to be prominent for smaller and larger viscosity contrasts, while they are relatively weak when viscosity contrast is close to one.

The presence of temperature variation (analogous to that of Wall and Wilson[65] in a rigid channel) on the pressure-driven flow in a slippery channel has been analyzed by Webber.[13] He has shown that boundary slip is stabilizing in the linear regime for a fixed value of slip parameter. The stability properties are enhanced with increasing temperature, but the critical Reynolds number decreases and then increases with temperature.

The present study aims to extend the investigations of Sahu and Govindarajan[18] and considers a linear stability of a symmetric three-layer pressure-driven flow of two miscible fluids in the presence of DD effect in a two-dimensional channel with slippery walls. Two fluids of different values of viscosity but same density occupy the core and the annular regions of the slippery channel. There is a mixed layer between the two fluids in which viscosity varies smoothly and is assumed to have an exponential dependence on the concentration of the solute species. The fluid in the core of the channel may be taken to be a pure solvent. The annular fluid contains the same solvent as that of the core fluid but has in it two solute species which are diffusing at different rates. The present investigation is also an extension of the SC system considered by Ghosh *et al.*[1] in a slippery channel. By a SC system, we mean the configuration where the viscosity stratification is achieved due to the presence of a single species or scalar either in one layer or in both the layers at different concentrations. Two-layer systems, with a layer of cold water and a layer of hot water or one layer of water and another layer of salty water or one layer at temperature T_1 and the other layer at temperature T_2 are some examples of SC systems. The results are expected to provide insight into the role of wall slip on the stability characteristics of the corresponding DD miscible two-fluid flow in a rigid channel as well as the influence of the presence of inhomogeneities in solute concentration of the two species with different diffusivities in a slippery channel. To the best of our knowledge, this is first attempt to understand the above mentioned effects.

It is hoped that the result will be useful in different applications as mentioned earlier. For example, if a PDMS (polydimethylsiloxane) channel is hosting a two-fluid flow of cold water and hot glycerol solution (where $R_s > 0$ and $R_f < 0$; R_s and R_f are log-mobility ratios of two scalars, namely, temperature and glycerol, defined later in Sec. II), then the present study provides details about the stability characteristics for the following two configurations. In the first configuration with $R_f + R_s < 0$, the flow system is inviscidly stable (Fig. 3; $R_f = -3.1$ and $R_s = 3.0$). But, according to the linear stability analysis (Sec. III), a new unstable mode (namely, DD-mode) is operational for low Reynolds numbers and this DD system is more unstable than the corresponding SC system (with cold and hot water).

On the other hand, for the configuration with $R_f + R_s > 0$, the DD-mode is absent but there is a big unstable region for a wide range of wave numbers due to the viscosity stratification.

The paper is organized as follows: The base state and the formulation of the linear stability equations are presented in Sec. II. The stability characteristics are discussed in Sec. III. The energy budget and the concluding remarks are given in Sec. IV and Sec. V, respectively.

II. MATHEMATICAL FORMULATION

A. Governing equations

We consider the two-dimensional pressure-driven laminar flow of two miscible, incompressible, Newtonian fluids in a plane channel of height $2H$, with velocity slip at the walls of the channel (as shown in Fig. 1). The two fluids have the same density ρ but viscosities are different. The core and annular regions of the channel are filled with fluids '1' and '2', respectively. Both the fluids contain the same solvent but have two species (S, F) diffusing at different rates. We refer to the one with higher diffusion rate $(\mathcal{D}_f)$ as F and the other as S with lesser diffusion rate $(\mathcal{D}_s)$. It is clear that the ratio $\delta = \frac{\mathcal{D}_f}{\mathcal{D}_s} \geq 1$. The concentrations of S and F in fluids '1' and '2' are S_1, F_1 and S_2, F_2, respectively. We use the Cartesian coordinate system (x, y) to model the flow dynamics, where x and y represent the streamwise and wall-normal directions, respectively. The walls of the channel with velocity slip are located at $y = \pm H$, and the centerline of the channel is at $y = 0$. As the flow is symmetric with respect to the centerline $(y = 0)$ of the slippery channel, the problem is formulated in the upper half of the channel for $0 \leq y \leq H$ (Fig. 1). There is a mixed layer of thickness 'q' between the two fluids occupying the region $h \leq y \leq h + q$.

The viscosity of the two fluids is assumed to depend exponentially on concentration of the solute species and is taken as[18]

$$\mu = \mu_1 \exp\left[R_s\left(\frac{S - S_1}{S_2 - S_1}\right) + R_f\left(\frac{F - F_1}{F_2 - F_1}\right)\right], \tag{1}$$

where $R_s = (S_2 - S_1)\frac{\partial}{\partial S}(\ln \mu)$ and $R_f = (F_2 - F_1)\frac{\partial}{\partial F}(\ln \mu)$ are the log-mobility ratios of the scalars S and F, respectively. We see from (1) that the basic viscosity is given by

$$\mu = \begin{cases} \mu_1 & \text{if } 0 \leq y \leq h, \\ \mu_m(y) & \text{if } h \leq y \leq h + q, \\ \mu_2 & \text{if } h + q \leq y \leq H, \end{cases} \tag{2}$$

where $\mu_2 = \mu_1 \exp(R_s + R_f)$ and $\mu_m(y) = \mu_1 \exp\left[R_s\left(\frac{S-S_1}{S_2-S_1}\right) + R_f\left(\frac{F-F_1}{F_2-F_1}\right)\right]$. Here, $\mu_m(y)$ gives the viscosity distribution in the mixed layer.

The flow dynamics is governed by the continuity, the Navier-Stokes, and the convection-diffusion equations for the two solute species. The boundary conditions at the centerline and at the

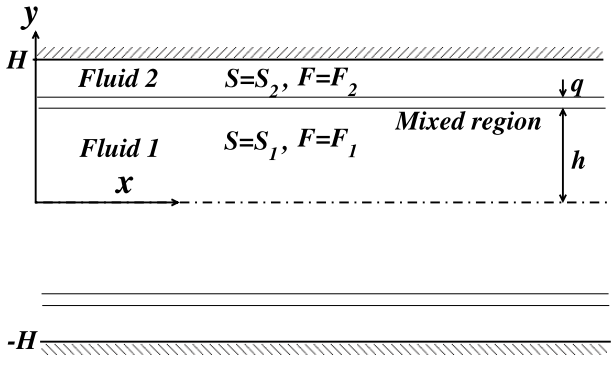

FIG. 1. Schematic of the flow system considered. The core and annular regions of the slippery channel contain the fluids '1' and '2', respectively. Here, fluid '1' occupies the region $-h \leq y \leq h$ and both the fluids are separated by a mixed layer of uniform thickness q. The slippery walls of the channel are located at $y = \pm H$.

slippery wall of the channel are

$$\frac{\partial u}{\partial y} = 0, \quad v = 0 \quad \text{at } y = 0, \tag{3}$$

$$u = -\beta_1 \frac{\partial u}{\partial y}, \quad v = 0 \quad \text{at } y = H, \tag{4}$$

where β_1 is the dimensional slip parameter and (u, v) is the velocity vector. The dimensionless governing equations and the boundary conditions are obtained using the following scales:

$$x^* = \frac{x}{H}, \quad y^* = \frac{y}{H}, \quad t^* = \frac{Q}{H^2}t, \quad (u^*, v^*) = \frac{H}{Q}(u, v), \quad p^* = \frac{H^2}{\rho Q^2}p, \quad \mu^* = \frac{\mu}{\mu_1},$$
$$h^* = \frac{h}{H}, \quad q^* = \frac{q}{H}, \quad m = \frac{\mu_2}{\mu_1}, \quad \beta = \frac{\beta_1}{H}, \quad s^* = \frac{S - S_1}{S_2 - S_1}, \quad f^* = \frac{F - F_1}{F_2 - F_1}, \quad \mu_m^* = \frac{\mu_m(y)}{\mu_1}, \tag{5}$$

where Q is the flow rate per unit distance in the spanwise direction, p is the pressure, and t is time. The dimensionless governing equations and boundary conditions (after suppressing $*$) are

$$u_x + v_y = 0, \tag{6}$$

$$u_t + uu_x + vu_y = \frac{\partial}{\partial x}\left[-p + \frac{2}{Re}\mu u_x\right] + \frac{\partial}{\partial y}\left[\frac{1}{Re}\mu(u_y + v_x)\right], \tag{7}$$

$$v_t + uv_x + vv_y = \frac{\partial}{\partial x}\left[\frac{1}{Re}\mu(u_y + v_x)\right] + \frac{\partial}{\partial y}\left[-p + \frac{2}{Re}\mu u_y\right], \tag{8}$$

$$s_t + us_x + vs_y = \frac{1}{Pe}[s_{xx} + s_{yy}], \tag{9}$$

$$f_t + uf_x + vf_y = \frac{\delta}{Pe}[f_{xx} + f_{yy}], \tag{10}$$

where $\mu = \exp\left[R_s s + R_f f\right]$, such that the values s and f are 0 and 1 for fluids '1' and '2', respectively. The boundary conditions are

$$u_y = 0, \quad v = 0 \quad \text{at} \quad y = 0, \tag{11}$$

$$u = -\beta u_y, \quad v = 0 \quad \text{at} \quad y = 1, \tag{12}$$

The above system is governed by the dimensionless parameters: the Reynolds number $Re = \rho Q/\mu_1$, the Péclet number $Pe = Q/\mathcal{D}_s$, the ratio of the diffusion coefficients of the species, $\delta = \mathcal{D}_f/\mathcal{D}_s$, the Schmidt number $Sc = Pe/Re$, and the dimensionless slip parameter $\beta = \beta_1/H$. For the faster diffusing fluid, the effective Schmidt number is Sc/δ.

B. Base state

The base state is obtained by solving the Eqs. (6)–(10) along with the boundary conditions (11) and (12) by assuming steady state and locally parallel flow

$$Re\left(\frac{dP_B}{dx}\right) = \frac{d}{dy}\left[\mu_B(y)\frac{dU_B(y)}{dy}\right]. \tag{13}$$

The solution of the above equation is given by

$$U_B(y) = \begin{cases} \dfrac{G}{2}\left[y^2 - h^2 + \dfrac{(h+q)^2 - 1 - 2\beta}{m} - 2\displaystyle\int_h^{h+q} \frac{y}{\mu_m(y)}\,dy\right] & \text{if } 0 \le y \le h, \\ \dfrac{G}{2}\left[\dfrac{(h+q)^2 - 1 - 2\beta}{m} - 2\displaystyle\int_y^{h+q} \frac{y}{\mu_m(y)}\,dy\right] & \text{if } h \le y \le h+q, \\ \dfrac{G}{2m}(y^2 - 1 - 2\beta) & \text{if } h+q \le y \le 1, \end{cases} \tag{14}$$

where $G = RePB_x$ and

$$\mu_B(y) = \begin{cases} 1 & \text{if } 0 \le y \le h, \\ \mu_m(y) = \exp\left[R_s\, s_B(y) + R_f\, f_B(y)\right] & \text{if } h \le y \le h+q, \\ m = \exp\left(R_s + R_f\right) & \text{if } h+q \le y \le 1. \end{cases} \tag{15}$$

Here, the subscript B designates the base state variables and s_B and f_B are taken to be a fifth order polynomial in the mixed layer,[18] such that the concentration profile is smooth up to the second derivative at $y = h$ and $y = h + q$

$$f_B(y) = s_B(y) = \begin{cases} 0 & \text{if } 0 \le y \le h, \\ \sum_{i=1}^{6} a_i y^{i-1} & \text{if } h \le y \le h+q, \\ 1 & \text{if } h+q \le y \le 1, \end{cases} \tag{16}$$

where $a_i, i = 1, 2, \ldots, 6$ are given by

$$\begin{aligned} a_1 &= -\frac{h^3}{q^5}(6h^2 + 15hq + 10q^2), \quad a_2 = \frac{30h^2}{q^5}(h+q)^2, \\ a_3 &= -\frac{30h}{q^5}(h+q)(2h+q), \quad a_4 = \frac{10}{q^5}(6h^2 + 6hq + q^2), \\ a_5 &= -\frac{15}{q^5}(2h+q), \quad a_6 = \frac{6}{q^5}. \end{aligned} \tag{17}$$

The concentration profiles defined in Eq. (16) can only be found at x location shorter than the solutal entry length. This implies that the analysis takes place at a point of the channel where the thickness of the mixed layer q is expected to grow up when increasing x. Therefore, the analysis that follows is based on a kind of "Frozen Time" approximation (see Appendix A for details). The dimensionless pressure-gradient is determined by requiring that $\int_0^1 U_B(y)dy = 1$. The base state velocity profiles are presented in Figs. 2(a)–2(d) for $R_s = 3.0$. Note that when $R_f + R_s > 0$, i.e., $m > 1$ ($R_f + R_s < 0$, i.e., $m < 1$) the highly (less) viscous fluid occupies the near wall (annular) regions of the channel. $R_f + R_s = 0$ ($m = 1$) corresponds to a system without viscosity stratification while when either $R_f = 0$ or $R_s = 0$, the system deals with continuously viscosity stratified SC fluid system of two miscible fluids. The above cases can be analyzed by fixing R_s and varying R_f or vice-versa. In this study, the thickness of the mixed layer is fixed as $q = 0.1$. As the Reynolds numbers considered in the present work are large, the Péclet numbers ($ScRe$ and $ScRe/\delta$) for the faster and slower diffusing species are also very large for $Sc > 1$. Thus, we assume to neglect the difference between the mixed layer thicknesses of the slower and faster diffusing species. It is noted that the aforementioned approximation may not be valid for $Sc \ll 1$. We also like to mention that, in reality, the thickness of the mixed layers for slower diffusing species (q_s) is different from that for the faster diffusing species (q_f). One can obtain q_f and q_s from direct numerical simulation or experiment. The order of magnitude analysis for the variation of the mixed layer thickness presented in Appendix A consider the diffusion of the individual species without incorporating the interaction between the two species. This yields $q_f = \sqrt{\delta} q_s$. The results for this case ($q_f \neq q_s$) are presented in Appendix B. The base state velocity $U_B(y)$ satisfies $U_B = -\beta(\partial U_B/\partial y)$ at $y = 1$ and $\partial U_B/\partial y = 0$ at $y = 0$. Figs. 2(a) and 2(b) present the base state velocity for $\beta = 0$ and $\beta = 0.1$, respectively, for $h = 0.7$ (i.e., the mixed layer located close to the channel wall). For the no-slip case ($\beta = 0$, Fig. 2(a)), the centerline velocity of the system with a high/less viscous fluid close to the wall ($R_f = -2.9/R_f = -3.1$) is more/less than that of the unstratified case ($R_f = -3.0$). The base state velocity at the mixed region increases with a decrease in R_f.

The velocity slip at the walls decreases the centerline velocity and increases the wall velocity for each value of R_f considered (Fig. 2(b), $\beta = 0.1$). The wall shear is less in case of slippery channel as compared to that in channel with no-slip boundary condition for each value of R_f used in

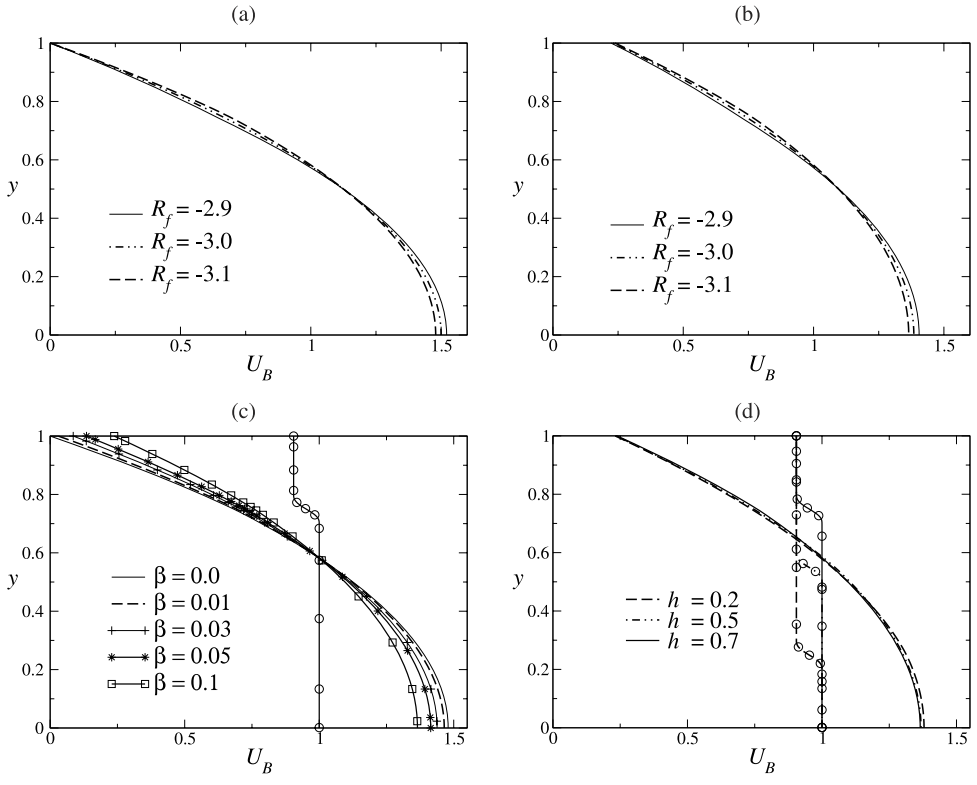

FIG. 2. Base state velocity and viscosity (with circle) profiles. Effects of R_f on velocity for $h = 0.7$; (a) $\beta = 0$; (b) $\beta = 0.1$. Effect of (c) the slip parameter β for $R_f = -3.1$, $h = 0.7$ and (d) the position of mixed layer h for $\beta = 0.1$, $R_f = -3.1$. In all panels, $R_s = 3.0$ and $q = 0.1$.

this figure. Also, the wall shear is smaller when a less viscous fluid is located close to the wall than that when a highly viscous fluid is adjacent to the wall.

Fig. 2(c) presents the base state velocity of the system with less viscous fluid close the wall ($R_f + R_s < 0$) for different values of the slip parameter (β). It can be seen that the centerline velocity decreases with increasing the value of slip parameter, and the role of slip is to reduce the wall shear. In the above system, the centerline velocity decreases slightly as the mixed layer of varying viscosity approaches the slippery wall (Fig. 2(d)). The corresponding base state viscosity profiles are plotted in Figs. 2(c) and 2(d). The location of the mixed layer (h) has no significant effect on the

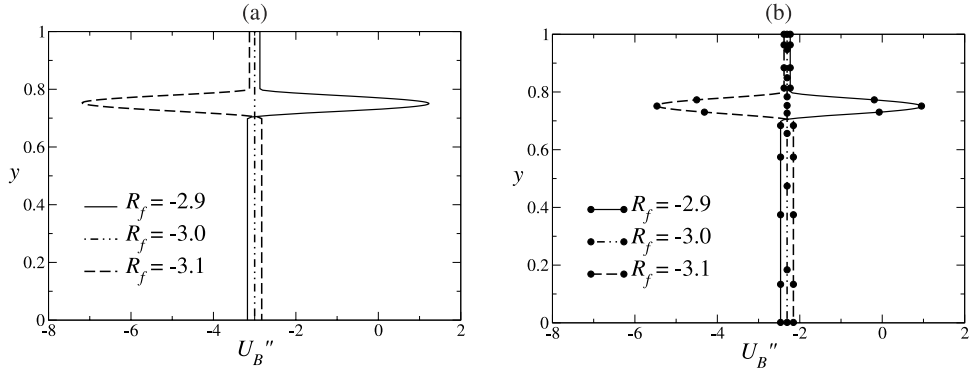

FIG. 3. Influence of R_f on $U_B''(y)$ when $R_s = 3.0$, $h = 0.7$, and $q = 0.1$; (a) the rigid channel case ($\beta = 0$) and (b) the slippery channel case ($\beta = 0.1$).

base state velocity for fixed values of other parameters (Fig. 2(d)), but it will be seen later that the stability characteristics of the system are highly influenced by varying h.

As information on $U_B''(y)$ is important in deciding the parameter values to be considered for the stability analysis in this study, Figs. 3(a) and (b) present the variation of $U_B''(y)$ for different values of R_f (fixing R_s) with $\beta = 0$ and $\beta = 0.1$, respectively. Fig. 3 enables one to infer whether the base state velocity profile has a point of inflection or not for the chosen values of other parameters. The point $y = \overline{y}$ at which $U_B''(\overline{y}) = 0$ gives the point of inflection for $U_B(y)$. The system with less viscous fluid near to the wall (dashed curve in Fig. 3(a) for $\beta = 0$) is inviscidly stable by Rayleigh's theorem[21] ($R_f = -3.1$, $R_s = 3.0$, $R_f + R_s < 0$), since the base velocity profile has no point of inflection. Now, for a configuration with $R_f + R_s > 0$ ($R_f = -2.9$, $R_s = 3.0$), $U_B''(y) = 0$ at two points (solid curve in Fig. 3(a) for $\beta = 0$). However, as the converse of Rayleigh's theorem is not true, no conclusion on the stability properties can be made for this configuration. As the slip parameter increases, the same trend as above is observed (Fig. 3(b) for $\beta = 0.1$). Note that the point of inflection lies in the mixed layer region ($h = 0.7$, $q = 0.1$). For the unstratified case ($R_f = -3.0$, $R_s = 3.0$), the flow system is inviscidly stable as $U_B''(y)$ does not change sign in the entire domain ($0 \le y \le 1$).

It is therefore of interest to see if the double-diffusive system with $R_f + R_s < 0$, which is inviscidly stable in the equilibrium state, remains stable or moves to an unstable state when an infinitesimal perturbation is imposed on it. In what follows, the governing Orr-Sommerfeld system is analyzed in detail for the case when the less viscous fluid occupies the region close to the slippery wall ($R_f + R_s < 0$, $R_s = 3.0$, $R_f = -3.1$). The effects of wall slip on the instabilities that occur for the no-slip case due to a small viscosity variation are examined using the values of R_f and R_s as mentioned above. Further, it is well known that when the less viscous fluid occupies the near wall region of the channel in a core-annular configuration, flow is stable in the context of single component flows.[31] In this study, the effects of wall-slip on the double-diffusive unstable mode in the configurations which are stable in the context of single component systems are investigated.

The slip parameter values used in the present study (β ranging from 0.01 to 0.1) are the same as those in the previous investigations[12,58–61,66] of a single fluid or immiscible two-fluid flow in a channel with velocity slip at the wall. In these studies, the slip parameter values are based on the review on the experimental investigations by Lauga *et al.*[67] This range of β can be realized for a flow in a hydrophobic channel of height ranging from 0.8 μm (40 μm) to 4 μm (200 μm) and corresponds to a slip length of 20 nm (40 nm).[1] The values in parentheses refer to the height of the hydrophobic channel and the corresponding slip length to achieve the slip parameter value $\beta = 0.1$ in a flow system.

C. Linear stability analysis

The temporal stability characteristics of the base flow ($U_B(y)$, $\mu_B(y)$, $P_B(x)$) described by Eqs. (14)–(17) are examined using a linear stability analysis by introducing an infinitesimal perturbation to the base flow. The flow variables are taken as the sum of the base state quantities and two-dimensional perturbations (designated by a hat) as

$$(u, v, p, s, f) = (U_B(y), 0, P_B(x), s_B(y), f_B(y)) + (\hat{u}, \hat{v}, \hat{p}, \hat{s}, \hat{f})(y) \exp\left[\mathrm{i}\,(\alpha x - \omega t)\right], \tag{18}$$

where $\mathrm{i} \equiv \sqrt{-1}$, α is the streamwise disturbance wave number, $\omega = \alpha c$ is the frequency of the two-dimensional disturbance, and c is the complex phase speed. In temporal stability analysis, α is real and ω is complex. The flow is linearly unstable if the imaginary part of ω, $\omega_i > 0$, and stable if $\omega_i < 0$, and neutrally stable if $\omega_i = 0$. The perturbation viscosity $\hat{\mu}$ is given by $\hat{\mu} = (\frac{\partial \mu_B}{\partial s_B}\hat{s} + \frac{\partial \mu_B}{\partial f_B}\hat{f})$. The velocity perturbations are expressed in terms of the stream function perturbation $\phi(= \hat{\phi}\exp(\mathrm{i}(\alpha x - \omega t)))$ such that $(\hat{u}, \hat{v}) = (\phi_y, -\phi_x)$. Modified Orr-Sommerfeld system is then derived from the dimensionless governing equations and the boundary conditions (6)–(12) using the standard procedure (see, e.g., Drazin and Reid[68]) and is given by (after suppressing hat (^) symbols)

$$\mathrm{i}\alpha\, Re\left[\phi''(U_B - c) - \alpha^2\phi(U_B - c) - U_B''\phi\right] = \mu_B\phi'''' + 2\mu_B'\phi''' + (\mu_B'' - 2\alpha^2\mu_B)\phi'' - 2\alpha^2\mu_B'\phi' + (\alpha^2\mu_B'' + \alpha^4\mu_B)\phi + U_B'\mu'' + 2U_B''\mu' + (U_B''' + \alpha^2 U_B')\mu, \tag{19}$$

$$i\alpha\, Pe\,[(U_B - c)s - s_B'\phi] = (s'' - \alpha^2 s), \tag{20}$$

$$i\alpha\, Pe\,[(U_B - c)f - f_B'\phi] = \delta(f'' - \alpha^2 f), \tag{21}$$

$$\phi' = -\beta\phi'', \quad \phi = s = f = 0 \quad \text{at} \quad y = 1, \tag{22}$$

$$\phi' = \phi''' = s' = f' = 0 \quad \text{at} \quad y = 0, \quad \text{(sinuous mode)} \tag{23}$$

where prime ($'$) denotes differentiation with respect to y. The above equations contain the terms that arise due to the continuous variations of the base flow velocity and viscosity perturbations. The system of Eqs. (19)–(23) constitutes an eigenvalue problem and determines the linear stability characteristics of infinitesimal two-dimensional disturbance in double-diffusive miscible three-layer pressure-driven flow in a channel with velocity slip at the walls. The classical Orr-Sommerfeld equation[68] can be recovered from the above equation by neglecting the terms due to viscosity stratification. The modified Orr-Sommerfeld system is solved numerically by the public domain software, LAPACK, after discretization of the domain using Chebyshev spectral collocation method (Canuto *et al.*[69]). The results are presented for sinuous mode (described by Eq. (23) at the centerline of the channel) as it was observed to be the dominant mode for the range of parameters considered. A sufficiently large number of grid points are taken in the mixed layer since the gradients are large in this layer. This is achieved by using the stretching function (Govindarajan[11])

$$y_j = \frac{a}{\sinh(by_0)}\,[\sinh\{(y_c - y_0)b\} + \sinh(by_0)], \tag{24}$$

where y_j are the locations of the grid points, a is the midpoint of the mixed layer, and y_c is a Chebyshev collocation point, given by

$$y_c = 0.5\left\{\cos\left[\pi\frac{(j-1)}{(n-1)}\right] + 1\right\} \tag{25}$$

and

$$y_0 = \frac{1}{2b}\ln\left[\frac{1 + (e^b - 1)a}{1 + (e^{-b} - 1)a}\right], \tag{26}$$

where n is the number of collocation points and b is the degree of clustering. In the present study, we performed our computations by taking $b = 8$ and using 121 collocation points. This gives an accuracy of at least five decimal places in the range of parameters considered.

III. RESULTS

The Orr-Sommerfeld system (19)–(23) shows that the stability properties of the flow system are influenced by the location of mixed layer (h), the velocity slip at the wall (β), ratio of diffusion coefficients of the species (δ), and the level of diffusivity (Sc). These effects are examined through the numerical solution of the modified Orr-Sommerfeld system. The accuracy and the correctness of the numerical code are assessed by first examining the critical Reynolds number (Re_{cr}) for the unstratified flow ($R_f = R_s = 0$) in a rigid ($\beta = 0$) and slippery ($\beta \neq 0$) channels. In the present analysis, the characteristic velocity scale corresponds to the average velocity in a channel, which is 2/3 times the maximum velocity in the channel. We observed that Re_{cr} for $\beta = 0$ is 3848.16 which is 2/3 times of the critical Reynolds number ($Re_{cr} = 5772.2$) based on the maximum velocity as a characteristic velocity.[68] When $\beta \neq 0$ (in slippery channel), the velocity scale chosen in the present study is $\frac{2}{3}(1 + 3\beta)$ times the maximum velocity of the no-slip case (which is the velocity scale chosen by Lauga and Cossu[61]). We observed that our result agrees well with the result of Lauga and Cossu[61] for $\beta \neq 0$ (same as Fig. 3 in Ghosh *et al.*[1]).

The computations are also performed for the SC case with velocity slip at the walls, in which a highly viscous fluid is placed adjacent to the wall ($m = 1.2$). This corresponds to $R_f = 0$ and $R_s = 0.1823$ in our computations. The results agree well with those obtained by Ghosh *et al.*[1] Having gained confidence based on the agreement of the available results in literature using the developed code, the computations are performed for the DD case for a range of parameter values that govern this system.

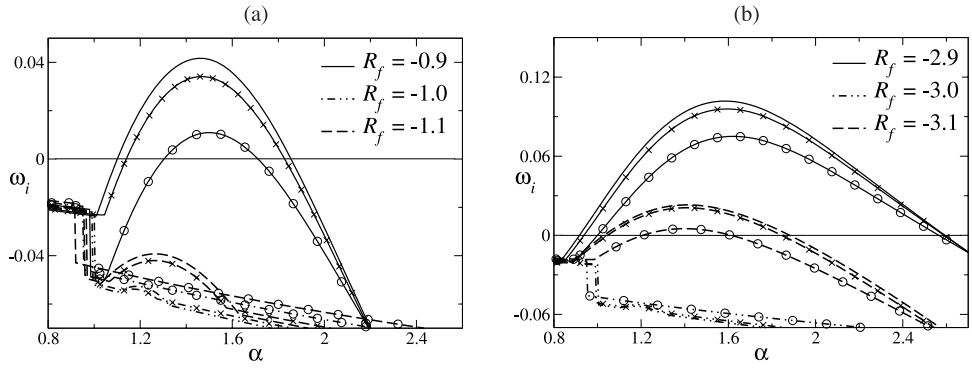

FIG. 4. Effects of R_f and slip parameter β on the growth rate (ω_i) as a function of wave number (α) for $Re = 1000$; (a) $R_s = 1.0$ and (b) $R_s = 3.0$. The curves with cross for $\beta = 0.01$ and with circle for $\beta = 0.05$. The curves without symbols represent no-slip case. Here, $Sc = 30$, $\delta = 10$, $h = 0.7$, and $q = 0.1$.

The growth rate (ω_i) for different values of R_f when $R_s = 1$ and $R_s = 3$ are plotted in Figs. 4(a) and 4(b), respectively. The other parameters are fixed at $Re = 1000, Sc = 30, \delta = 10, h = 0.7$, and $q = 0.1$. The influence of β on the growth rate is also assessed. The configuration with $R_f + R_s > 0$ ($R_s = 1, R_f = -0.9$) has positive growth rate, while that with $R_f + R_s \leq 0$ exhibits negative growth rate (Fig. 4(a)). An increase in R_s (to $R_s = 3$) and decrease in R_f (Fig. 4(b)) display a positive growth rate for the cases $R_f + R_s \gtrless 0$ and a negative growth rate for $R_f + R_f = 0$. We observed from Figs. 4(a) and 4(b) that the role of slip parameter (β) is to reduce the growth rate and the range of unstable wave numbers (α). This suggests that we investigate in detail the neutral stability boundaries and the critical Reynolds numbers for onset of instability for the case when $R_s = 3$ and R_f takes values -2.9, -3.0, and -3.1. This would include the configurations for which $R_f + R_s > 0$ and $R_f + R_s < 0$.

Now, in the case of $R_f + R_s > 0$ (when $R_s = 3$ and $R_f = -2.9$), we study the effects of the inertia as well as the slip parameter. Fig. 5(a) presents the neutral stability maps for different values of β. The other parameters are same as those used in Fig. 4(b). We see that a large unstable region appears for a wide range of wave numbers similar to that for a SC case due to viscosity stratification under overlap condition ($h = 0.7$). The zoom of the region close to the onset of instability is presented in Fig. 5(b) and we found that β has a destabilizing effect. We infer from Figs. 4(b), 5(a), and 5(b) that the configuration with $R_f + R_s > 0$ ($R_f = -2.9, R_s = 3.0$) is destabilizing as β increases but the range of unstable wave numbers (α) decreases with an increase in β at higher Reynolds numbers.

The base state profiles for the configuration with $R_f + R_s < 0$, where $R_s = 3$ and $R_f = -3.1$ are inviscidly stable for all values of slip parameter (β) considered in this investigation (Fig. 3). It is

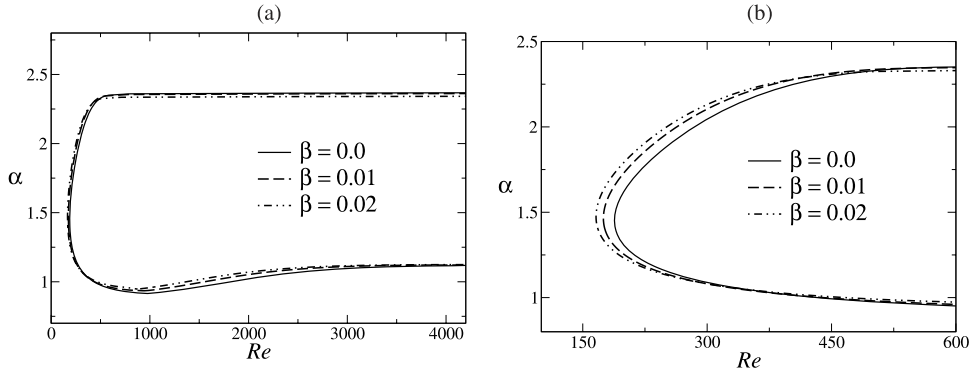

FIG. 5. Neutral stability curves for $R_s = 3$, $R_f = -2.9$, $Sc = 30$, $\delta = 10$, $h = 0.7$, and $q = 0.1$; (a) effect of slip parameter β; (b) zoom of the region $100 \leq Re \leq 600$ in Fig. 5(a).

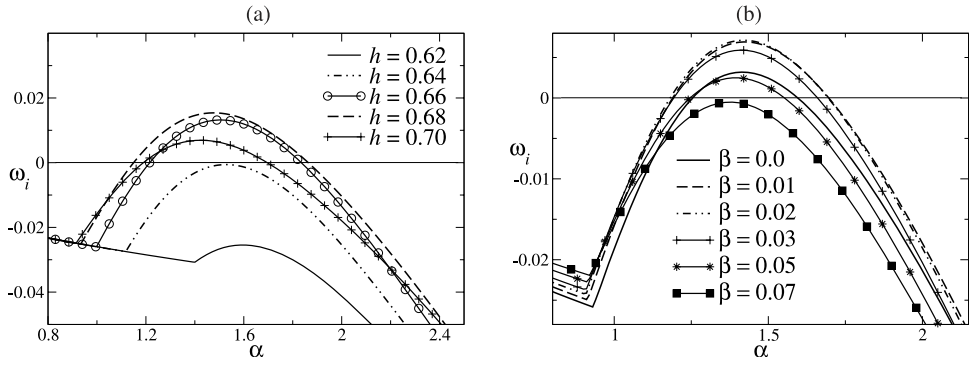

FIG. 6. Influence of various flow parameters on the growth rate (ω_i) in $\alpha - \omega_i$ plane for $Re = 650$, $R_s = 3.0$, $R_f = -3.1$, $Sc = 30$, $\delta = 10$, and $q = 0.1$; (a) effect of h for $\beta = 0.01$ and (b) effect of β for $h = 0.7$.

of interest to see whether such a stable base state remains stable even after the perturbations are introduced. In view of this, we pursue our computations in detail for the case $R_f + R_s < 0$.

The effects of the location of the mixed layer (h) and the slip parameter (β) on the growth rate are examined in Figs. 6(a) and 6(b) for the configuration with $R_f + R_s < 0$ ($R_s = 3.0, R_f = -3.1$). The rest of the parameters are $Re = 650$, $Sc = 30$, $\delta = 10$, and $q = 0.1$ with $\beta = 0.01$ (for Fig. 6(a)) and $h = 0.7$ (for Fig. 6(b)) It is clear from Fig. 6(a) that when the mixed layer approaches towards the slippery wall, the growth rate increases with an increase in h (up to $h = 0.68$) but with further increase in h the growth rate decreases. Inspection of Fig. 6(b) reveals that under the overlap condition (for $h = 0.7$), the growth rate exhibits a nonmonotonic behaviour with respect to the slip parameter β.

The neutral stability maps are presented in Figs. 7(a)–7(f) for $R_f + R_s < 0, Sc = 30, \delta = 10$, and $q = 0.1$. The Tollman Schlichting (TS) mode instability occurs at large Reynolds numbers and small wave numbers. It is the only mode of instability for $h = 0.60$ and $h = 0.62$ (Fig. 7(a); $R_s = 3, R_f = -3.1, \beta = 0.01$). The critical Reynolds number (Re_{cr}) exhibits a nonmonotonic behavior with respect to h. As the location of the mixed layer approaches the slippery wall, we see that apart from the TS-mode of instability, a new mode of instability also occurs (referred to as the DD mode) similar to that observed by Sahu and Govindarajan[18] for flow in a rigid channel. This mode occurs at low Reynolds numbers and for a wide range of wave numbers. This new mode of instability (DD) is absent for $h < 0.65$ when $\beta = 0.01$ while for $\beta = 0$, it occurs for $h = 0.62$.[18] This shows that for the occurrence of the DD mode instability, the mixed layer has to be placed closer to the wall in the case of a slippery channel than in the case of a channel with rigid walls. As h increases to $h = 0.7$, it can be seen in Fig. 7(a) that the critical Reynolds number for DD mode increases. Increasing h delays, the onset of instability of the DD mode but increases the range of unstable wave numbers and the region of instability. The effects of wall slip on the DD mode are examined in Fig. 7(b) when $h = 0.7$. We see that although the critical Reynolds number (Re_{cr}) decreases up to $\beta = 0.02$, the unstable region shrinks and the range of unstable wave numbers decreases. Beyond $\beta = 0.03$, Re_{cr} value increases and the role of slip at the walls is to stabilize the flow system.

It is interesting to see that although the above configuration ($h = 0.7$) in the SC system in a slippery channel with less viscous fluid close to the wall ($m < 1$) is stable for all wave numbers and small Reynolds numbers, it becomes unstable in the presence of two species (DD system with $R_f + R_s < 0$). This is due to the occurrence of the DD mode. It is also evident from the results presented in Fig. 7(c) (for $h = 0.60$) that the slip parameter, β stabilizes the TS mode.

If we choose $R_f = 3.0$ and $R_s = -3.1$ (still $R_f + R_s < 0$), the stability characteristics are the same as described above, but the DD mode occurs when the mixed layer is more closer to the slippery walls (see Fig. 7(d) for $h = 0.7, \beta = 0.01$). A smaller unstable region appears at lower Reynolds numbers as compared to that observed for $R_f = -3.1$ and $R_s = 3.0$ (Fig. 7(a)). In this case (for $R_f = 3.0$ and $R_s = -3.1$) also the DD and TS modes are stabilized by the presence of slip at the walls (see Fig. 7(e) for $h = 0.7$ and Fig. 7(f) for $h = 0.60$; $R_f = 3.0, R_s = -3.1, Sc = 30$, and $\delta = 10$).

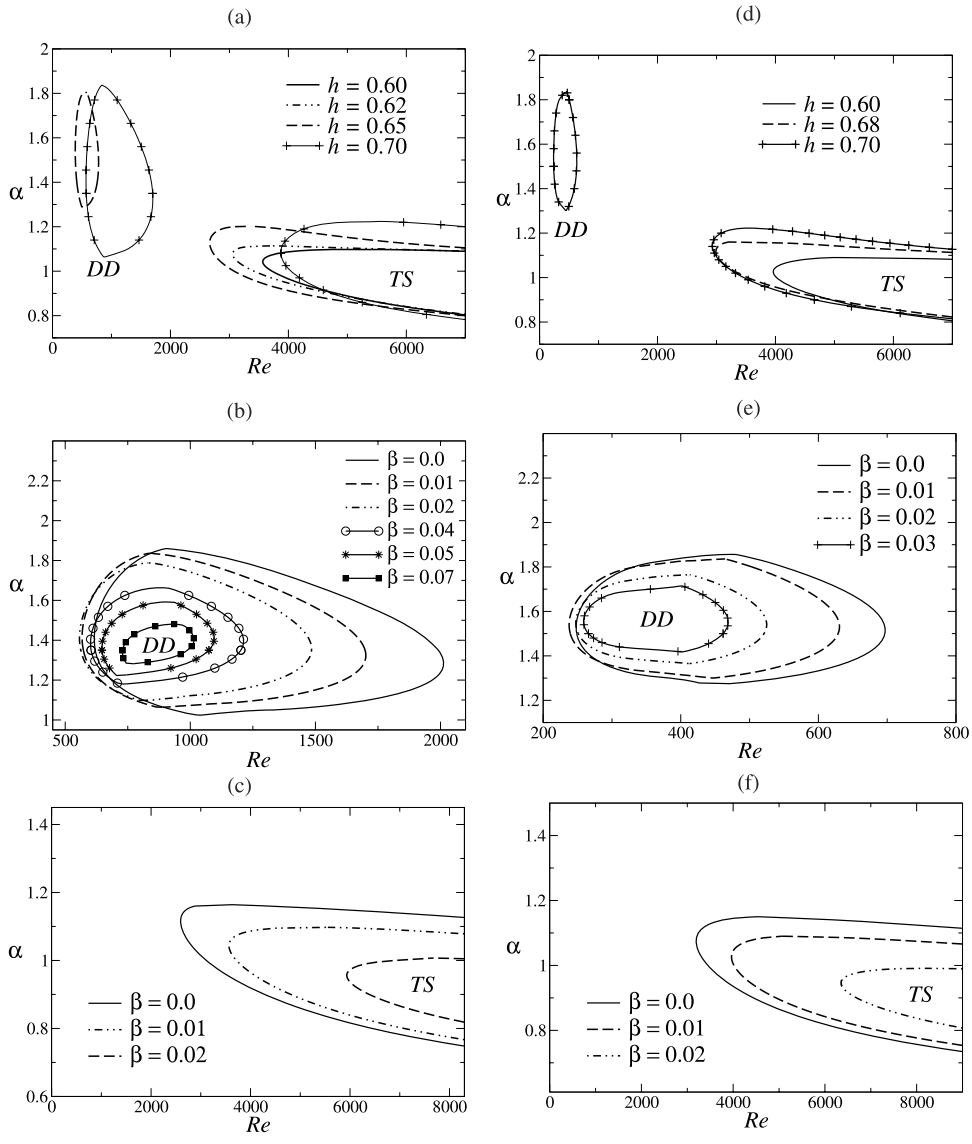

FIG. 7. The neutral stability boundaries for $R_s = 3.0$, $R_f = -3.1$ in (a)–(c) and for $R_s = -3.1$, $R_f = 3.0$ in (d)– (f). All other parameters are as $Sc = 30$, $\delta = 10$, and $q = 0.1$. Panels (a) and (d) contain effects of h for $\beta = 0.01$. Panels (b) and (e) show effect of β on the DD-mode for $h = 0.7$. At last, panels (c) and (f) represent the effect of β on the TS-mode for $h = 0.6$.

The effects of variations in the thickness of the mixed layer (q) on the stability characteristics is displayed in Fig. 8 for $R_s = 3.0, R_f = -3.1, h = 0.7, Sc = 30, \delta = 10$, and $\beta = 0.01$. We see that increasing q does not alter the stability characteristics qualitatively, namely, the occurrence of the unstable DD and TS modes. Further, an increase in q stabilizes the DD as well as the TS mode by increasing the critical Re and decreasing the bandwidth of unstable wave numbers. For the DD mode, unstable region shrinks and extends to higher Reynolds numbers.

The effects of the location of the mixed layer on the critical Reynolds number (Re_{cr}) for the TS mode and the DD mode are presented in Figs. 9(a) and 9(b), respectively. The effect of the slip parameter on Re_{cr} for each of these modes is also assessed. The other parameters are fixed as $R_f = -3.1, R_s = 3.0, Sc = 30, \delta = 10$, and $q = 0.1$. Fig. 9(a) shows that, in the case of a rigid channel, the TS mode is stabilized as the mixed layer approaches the wall as indicated by increase in critical values of Re as h increases. On the other hand, for a flow in a slippery channel, the critical Reynolds number decreases up to some value of h and beyond this, it increases. The decrease is

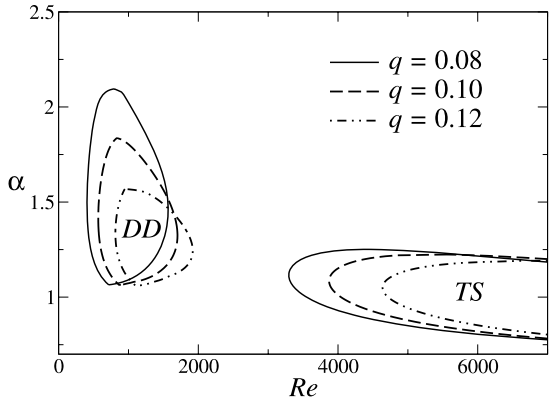

FIG. 8. Effects of mixed layer thickness (q) on the stability boundaries for $R_s = 3.0$, $R_f = -3.1$, $h = 0.7$, $Sc = 30$, $\delta = 10$, and $\beta = 0.01$.

significant for higher values of β. For any $h < 0.7$, the critical Re increases with increase in β thereby indicating the stabilizing role of β on TS mode, for these locations of the mixed layer. For $h > 0.7$, when $\beta = 0.01$, the TS mode is slightly destabilized. For a fixed β, critical Reynolds number for the DD mode (Fig. 9(b)) increases as the mixed layer approaches the rigid/slippery wall ($\beta = 0/\beta \neq 0$). For smaller values of h, the DD mode for flow in a slippery channel is more stable than that in a rigid channel. The appearance of the DD mode is delayed with an increase in β, as observed in Fig. 7(a), is also confirmed in Fig. 9(b). The location of the mixed layer where the flow in a slippery channel becomes more unstable than that in a rigid channel, moves closer to the slippery wall as β increases.

The effects of δ, the ratio of diffusion rates are examined in Fig. 10 when $Sc = 30, R_s = 3$, $R_f = -3.1, h = 0.7$, and $q = 0.1$. We see that the DD mode is absent for $\delta = 1$ ($\mathcal{D}_f = \mathcal{D}_s$), which corresponds to a SC two fluid miscible case in a slippery channel (Fig. 10(a); $\beta = 0.01$). In this case, the only mode of instability is the TS-mode, appearing at higher Reynolds numbers and $O(1)$ wave numbers. With an increase in δ, there occurs two distinct modes of instability occupying distinct regions in the $\alpha - Re$ plane, namely, the DD mode and the TS mode. The DD mode appears at moderate Reynolds numbers and moderate wave numbers. As δ increases, the TS mode is stabilized as but the DD mode is destabilized as is evident from the reduction in critical Reynolds number values. The unstable region enlarges with increase in δ for the DD mode. The range of unstable wave numbers also increases with an increase in δ. Figs. 10(b) and 10(c) depict the critical Reynolds number (Re_{cr}) as a function of δ for different values of slip parameters, for the TS and the DD mode, respectively. The other parameters are the same as in Fig. 10(a). In the region below any curve in the $\delta - Re_{cr}$ plane (Figs. 10(b) and 10(c)), the amplitude of the perturbations decays

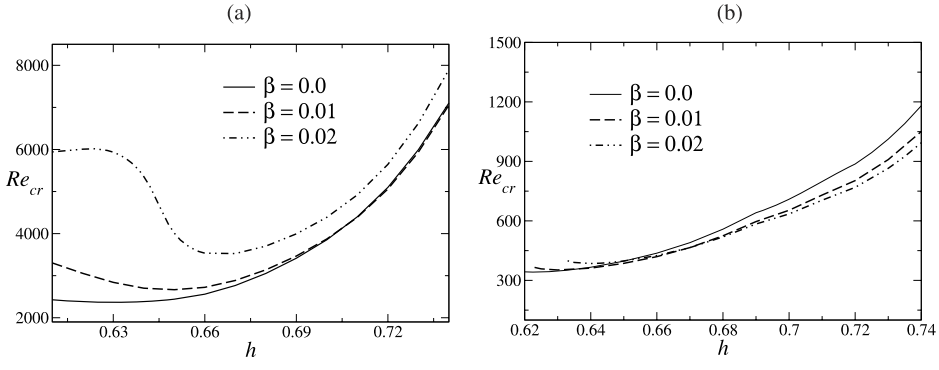

FIG. 9. The critical Reynolds number (Re_{cr}) as a function of h for $R_s = 3.0$, $R_f = -3.1$, $Sc = 30$, $\delta = 10$, and $q = 0.1$; (a) β effect on Re_{cr} for TS-mode and (b) β effect on Re_{cr} for DD-mode.

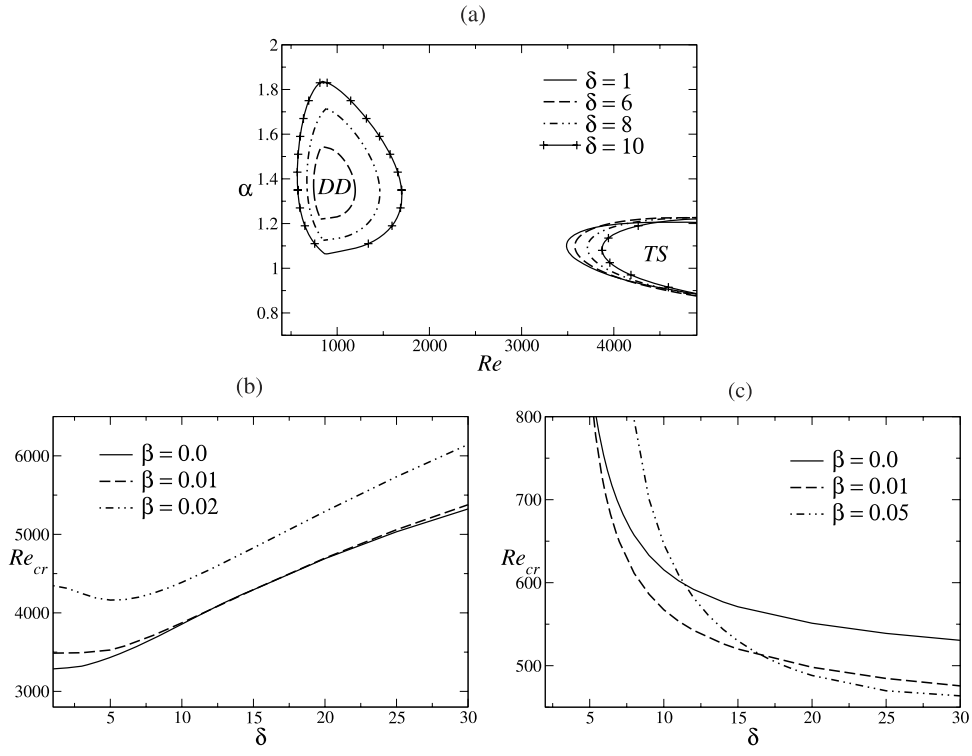

FIG. 10. Influence of the ratio of diffusion rates δ on the neutral stability boundaries and the critical Re values (Re_{cr}) for $R_s = 3.0$, $R_f = -3.1$, $Sc = 30$, $h = 0.7$, and $q = 0.1$; (a) stability curves for different δ with $\beta = 0.01$; effects of β on critical Re as a function of δ (b) for TS-mode and (c) for DD-mode.

and therefore is a stable region. For a fixed β, the critical Reynolds number decreases initially for small values of δ. Beyond some value of δ, it increases monotonically, which reveals the stabilizing role exhibited by δ on the TS mode (Fig. 10(b)). As β increases, at a fixed δ, the critical Re (Re_{cr}) for the TS mode increases indicating the stabilizing effect of the slip parameter β. For a fixed β, the Re_{cr} for the DD mode, however, decreases with increase in δ (Fig. 10(c)) showing the destabilizing effect of δ on the DD mode of instability. But, the slip parameter β has a dual role on the DD mode instability. For small values of β (say $\beta = 0.01$), the critical Re, at any fixed δ is less than that for $\beta = 0$, suggesting that the slip has a destabilizing effect. However, as β increases to $\beta = 0.05$, the critical Reynolds number increases up to a certain value of δ and after that it decreases with increase in δ. There is a critical value of δ, for $\beta \neq 0$ beyond which the DD mode is more unstable than that for a flow system in a rigid channel ($\beta = 0$). Also, as the slip parameter increases, the occurrence of the DD mode begins to appear at a higher δ.

It is interesting to see that as Schmidt number (Sc, the diffusivity parameter) increases, the critical Reynolds number decreases for the DD mode but the unstable region shrinks with increase in Sc (Fig. 11(a); $\beta = 0.01, R_f = -3.1, R_s = 3.0, \delta = 10, h = 0.7$, and $q = 0.1$). Also, for the TS mode, the critical Re decreases with an increase in Sc but the range of wave numbers increases. From Fig. 11(b) (all parameters are the same as in Fig. 11(a)), we see that the above scenario for the TS mode is observed for a wide range of Sc for a flow in a rigid/slippery channel. The slip parameter β has a stabilizing effect on the TS mode for the range of Sc considered in Fig. 11(b).

The critical Re value (Re_{cr}) as a function of Sc for the DD mode is presented in Fig. 11(c) (with set of parameters are the same as in Fig. 11(a)) for different values of β. As Sc increases, the critical Reynolds number (Re_{cr}) decreases with an increase in β. Further, for all values of β considered, the critical Re decreases with increase in Sc indicating the destabilizing effect of Sc.

The critical Reynolds number as a function of R_f for the TS mode is presented in Fig. 12(a) ($R_s = 3.0, Sc = 30, h = 0.7, q = 0.1$) for both the cases $R_f + R_s > 0$ and $R_f + R_s < 0$ (when $\delta = 1$ and 10). We see that at $R_f = -3.0$, the critical Reynolds number value of 3848.16 is recovered

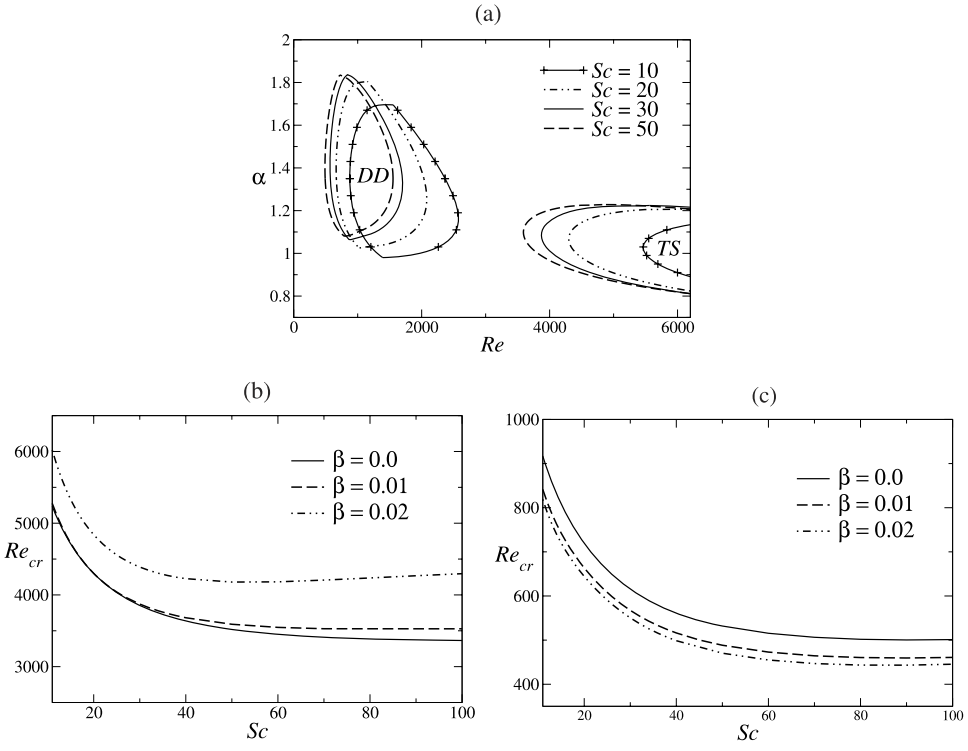

FIG. 11. Influence of diffusivity parameter Sc on the neutral stability boundaries and the critical Re values (Re_{cr}) for $R_s = 3.0$, $R_f = -3.1$, $\delta = 10$, $h = 0.7$, and $q = 0.1$; (a) stability curves for different Sc with $\beta = 0.01$; β effects on critical Re in the $Sc - Re_{cr}$ plane (b) for TS-mode and (c) for DD-mode.

for $\delta = 1$ and $\beta = 0$ (single fluid flow in a rigid channel with constant viscosity) agrees with $\frac{2}{3}$ times the critical Reynolds number obtained by Drazin and Reid[68] using maximum velocity in the channel as the velocity scale. The corresponding result in a slippery channel (for $\delta = 1, \beta = 0.01$) also agrees with the result presented by Lauga & Cossu[61] and it is $\frac{2}{3}(1 + 3\beta)$ times the critical Reynolds number obtained by Lauga & Cossu.[61] The stability characteristics of the TS mode for $\delta = 1$ and $\delta = 10$ are qualitatively similar with respect to R_f. However, when $\delta = 10$, the TS mode is more stable till $R_f = -3.0$ and less stable beyond $R_f = -3.0$ for flow in both rigid and slippery channels. This exchange of stability occurs at the critical Reynolds number for the flow of a single fluid with constant viscosity in a rigid/slippery channel, respectively. The role of β is to promote

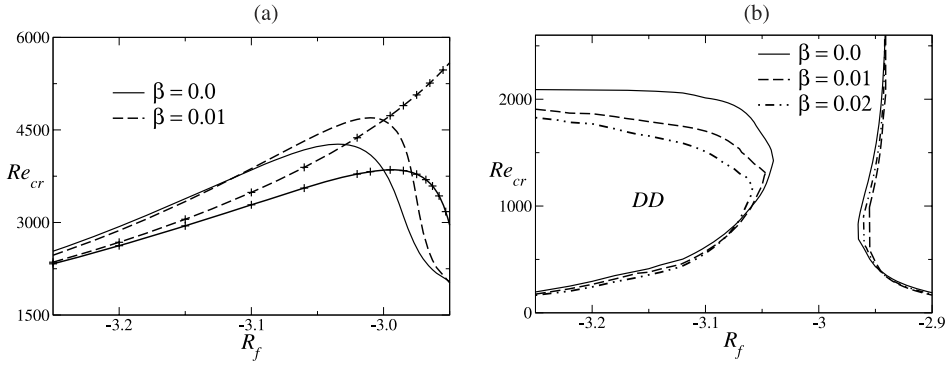

FIG. 12. Effects of slip parameter, β on the critical Reynolds number (Re_{cr}) as a function of R_f for $R_s = 3.0$, $h = 0.7$, $Sc = 30$, and $q = 0.1$; (a) for TS-mode, with symbols ($\delta = 1$) and without symbols ($\delta = 10$), (b) for DD-mode ($\delta = 10$).

the stabilizing effect on the TS mode for $\delta = 1$, whereas for $\delta = 10$, β ($\beta = 0.01$) has a dual role depending on R_f.

The details about the behaviour of the DD mode instability is presented in Fig. 12(b) (the critical Re as a function of R_f for the DD mode with different β, other parameters are the same as in Fig. 12(a)). The unstable region for the DD mode is a closed region (as seen in Figs. 7, 10(a), and 11(a)). As a result, the bounds on the Reynolds number (minimum and maximum Re) within which the unstable region for the DD mode lies are presented in this figure. The results reveal that at the lower branch (for minimum Re), the DD mode is destabilized as β increases (up to $\beta = 0.02$), while the reverse trend is noted in the upper branch (for maximum Re). From Fig. 12(b), we also infer that as R_f decreases from $R_f = -3.0$, the occurrence of the DD mode is delayed by the presence of velocity slip at the wall. When $R_f = -2.9$, we have seen in Fig. 5(a), an unstable region extending from low Reynolds number to high values for a wide range of wave numbers. If now R_f is varied so that $R_f + R_s > 0$ and observe the corresponding critical Reynolds numbers, we see that there is an unstable region for $R_f > -3.0$ in Fig. 12(b). This may be attributed to overall effects of viscosity stratification in the flow system in a channel. It is interesting to see that, in this case, the effects of slip parameter are similar to that for the DD mode (Fig. 12(b)).

The above results show that the effects of wall-slip on the DD mode is remarkable and unexpected. Sec. IV provides an explanation of both the stabilizing and destabilizing effects of slip on the double-diffusive instability through an energy budget analysis.

IV. ENERGY BUDGET ANALYSIS

The Reynolds-Orr energy equation[21,68] explains the key mechanism, where the interaction of the perturbations with the base flow and viscous dissipation of kinetic energy is responsible for the change of disturbance energy for Poiseuille flow in a channel with no-slip at the walls. For Poiseuille flow in a channel with velocity slip at the channel walls, Ren and Xia[63] have derived the generalized Reynolds-Orr energy equation incorporating the effects of wall slip. The results show that for very weak slip effects, the disturbance energy transferred from the base flow to perturbation overcomes the viscous dissipation. As a result, the disturbance energy grows indicating the destabilizing effects of wall slip. For higher values of slip parameter, wall slip shows stabilizing effects since there is a decay of disturbance energy due to viscous dissipation overcoming the energy production. It is important to note that viscosity of the fluid is a constant in this case.

The present study deals with stability of a double-diffusive two fluid flow in a slippery channel across which viscosity varies smoothly (as given by Eqs. (15)–(17) in the manuscript) and the analysis accounts for viscosity perturbations. In what follows, the modified-generalized Reynolds-Orr energy equation is derived and the energy budget in the perturbed slip flow is examined. The physical mechanism of the dual role of the velocity slip at the wall (as stabilizing or destabilizing) on the double-diffusive instability is then explained by considering an energy budget analysis. We take the inner product of the x and y momentum equations for the perturbations with the perturbation velocity components in the x and y directions, respectively. The resulting equations are then added, and the final equation is integrated over the control volume. The volume integrals are converted to surface integrals using divergence theorem and simplified. Considering the x-direction integration over a unit wavelength and y-direction integration between the centerline and the slippery wall, the following modified-generalized Reynolds-Orr energy equation is obtained (after using normal mode for perturbations):

$$E_t^* = RES^* + DIS^* + A^* + B^* + B_x^* + B_y^*, \tag{27}$$

where

$$E_t^* = \frac{\omega_i}{2}\int_0^1 (|\phi'|^2 + \alpha^2|\phi|^2)dy,$$

$$RES^* = -\frac{i\alpha}{4}\int_0^1 U_B'(\bar{\phi}\phi' - \phi\bar{\phi}')dy,$$

$$DIS^* = -\frac{1}{2Re}\int_0^1 \mu_B\left(|\phi''|^2 + 2\alpha^2|\phi'|^2 + \alpha^4|\phi|^2\right)dy - \frac{\beta}{2Re}\left[\left(\mu_B|\phi''|^2\right)\Big|_{at\ \ y=1}\right],$$

$$A^* = \frac{\alpha^2}{2Re}\int_0^1 \mu_B{}'\left(\phi\bar{\phi}' + C.C.\right)dy, \quad B^* = \frac{1}{4Re}\int_0^1 U_B{}''\left(\mu\bar{\phi}' + C.C.\right)dy,$$

$$B_x^* = -\frac{\alpha^2}{4Re}\int_0^1 U_B{}'\left(\mu\bar{\phi} + C.C.\right)dy, \quad B_y^* = \frac{1}{4Re}\int_0^1 U_B{}'\left(\mu'\bar{\phi}' + C.C.\right)dy.$$

In the above equations (Eq. (27)), an over-bar ($\bar{}$) represents the complex conjugate ($C.C.$), and E_t^* is the time rate of change of the total disturbance energy; RES^* is the rate of energy transfer between the base flow and the disturbance (commonly known as "Reynolds stress" term); DIS^* is the energy due to viscous dissipation; A^* corresponds to contribution to energy of the disturbance from the y-gradient of base viscosity; B^*, B_x^*, and B_y^* are related to contributions arising from the perturbation viscosity, gradients of viscosity perturbation in the x and y directions, respectively.

It is to be noted that Eq. (27) contains not only the terms RES^* and DIS^* (that appear in the classical Reynolds-Orr energy equation[21,68] for Poiseuille flow in a rigid channel and in the generalized Reynolds-Orr energy equation presented by Ren and Xia[63] for the same flow in a channel with wall slip) but also the other terms A^*, B^*, B_x^*, and B_y^*. Each term in Eq. (27) is influenced by the wall slip either due to the dependence of the base velocity on the slip parameter or due to the influence of velocity slip on the velocity perturbations.

Normalising Eq. (27) with $\frac{1}{2}\int_0^1(|\phi'|^2 + \alpha^2|\phi|^2)dy$ yields

$$E_t = RES + DIS + A + B + B_x + B_y, \tag{28}$$

where E_t is nothing but the growth rate (ω_i). This choice of normalising simplifies the interpretation of the variations of the different terms in the energy balance Eq. (27) and makes the relative contributions comparable. Attention is focused on the range of unstable wave numbers for the DD-mode instability for different values of slip parameter. As discussed previously, the flow system is stable or unstable if $E_t < 0$ or $E_t > 0$, respectively. We have ensured the accuracy of our computations by considering each term in Eq. (28) independently and it is found that the left and the right hand sides of Eq. (28) are equal up to five decimal places.

Fig. 7(b) in the paper shows that the critical Reynolds number for the DD-mode for $\beta = 0.01$($\beta = 0.07$) is less (more) than that for $\beta = 0$ indicating the destabilizing (stabilizing) role of slip. This can be explained by the energy budget Eq. (28) as follows. As our interest is in the threshold for instability, the terms that appears in Eq. (28) corresponding to the present problem with slip effects incorporated must be compared with the corresponding terms for the no-slip stable state. The critical Reynolds number for the no-slip case with $R_s = 3.0$, $R_f = -3.1$, $Sc = 30$, $\delta = 10, h = 0.7$, and $q = 0.1$ is $Re \simeq 623$ and it occurs at $\alpha \simeq 1.41$. In view of this, Fig. 13 presents the different terms in Eq. (28) as a function of wave number (α) for $Re = 623$ with the rest of the parameters the same as those mentioned above.

Fig. 13(a) shows that E_t or ω_i is positive for a range of α values for $\beta = 0.01$ (dashed line). However, E_t is negative for all α values when $\beta = 0.07$ (dashed-dotted line). So, E_t exhibits a non-monotonic behaviour with an increase in β. DIS term is always negative (Fig. 13(b)) and is a decreasing function of α for all values of β considered. So, there is a damping of disturbance kinetic energy induced by DIS. An increase in β causes an increase in DIS. The disturbance energy production term RES is always positive for all β values considered (Fig. 13(g)) and therefore contributes to destabilization of the flow system. The terms B and B_x are negative always (Figs. 13(d) and 13(e)) and they also decrease as α increases; however they are small as compared to other terms. The terms A and B_y are both positive (Figs. 13(c) and 13(f)) and increase with an increase in α (note that A attains a maximum and then decreases beyond a certain wave number). The contribution from the term A is very small for any value of β considered. B_y, being positive, contributes to destabilization of the flow system. It is important to note that all components (terms in Eq. (28)) that contribute to energy transfer are affected by the wall slip (β), and therefore they are responsible for the stabilizing or destabilizing effects of wall slip β.

A close inspection of RES (Figs. 13(g) and 13(h)) reveals that there is a nonmonotonic behaviour of RES with respect to slip β. For smaller values of α, RES is more for $\beta = 0.01$ than that for

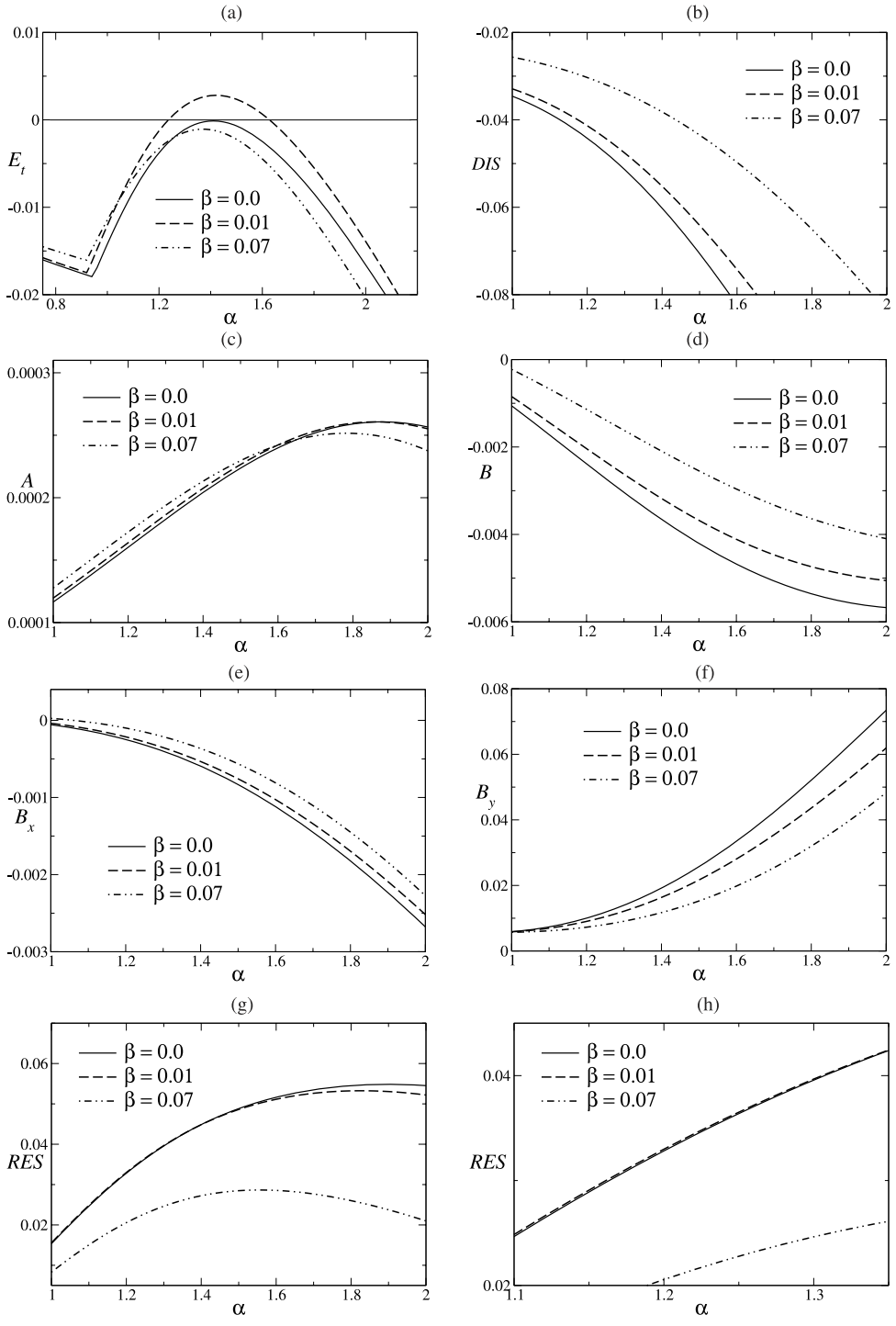

FIG. 13. Variation of E_t, DIS, A, B, B_x, B_y, and RES with α for $Re = 623$ are shown in panels (a)-(g), respectively. The other parameters are $R_s = 3.0$, $R_f = -3.1$, $Sc = 30$, $\delta = 10$, $h = 0.7$, and $q = 0.1$. Panel (h) shows the zoomed picture of panel (g).

$\beta = 0$ (see Fig. 13(h)). Beyond $\alpha(\simeq 1.41)$, RES for $\beta = 0.01$ is less than that for $\beta = 0$. However, for $\beta = 0.07$, RES is always less than that obtained $\beta = 0$.

The disturbance energy that arises due to RES, A, and B_y (which are positive and hence have a destabilizing effect) for $\beta = 0.01$ overcomes the disturbance energy that arises due to DIS, B, and

B_x (which are negative and hence have a damping effect), which causes positive growth rate in E_t (Fig. 13(a)). On the other hand, for $\beta = 0.07$, the damping effect due to DIS, B, and B_x overcomes the destabilizing contributions from RES, A, and B_y and this is responsible for the negative growth rate in E_t (Fig. 13(a)). This clearly explains the dual role of wall slip at the onset of instability of the DD mode.

V. CONCLUSIONS

A linear stability analysis of a DD two-fluid flow in a slippery channel has been considered. It exhibits strikingly different stability characteristics as compared to the corresponding SC miscible two-fluid flow in a slippery channel. While a configuration with less viscous fluid close to the slippery wall ($m < 1$) is more stable in the SC system, in the DD system with $R_f + R_s < 0$ ($m < 1$), it is unstable. This is due to the occurrence of a new unstable mode (the DD-mode) at low Reynolds numbers and a wide range of wave numbers (due to DD effects). Such a mode exists under overlap conditions (i.e., mixed layer overlapping the critical layer of dominant disturbance) due to different diffusion rates of the two species in the miscible two-fluid flow. The slip parameter has both stabilizing as well as destabilizing effects on the stability of the DD system. In fact, the results reveal that for higher values of β, the critical Reynolds number increases and the range of unstable wave numbers decreases thereby shrinking the unstable region for the dominant DD mode. This shows that a DD system in a slippery channel is more stable than the corresponding DD system in a rigid channel. Also, it is possible to find a region in the $\alpha - Re$ space (for small values of slip parameter β), in which the DD system in a slippery channel is more unstable than that in a rigid channel (due to lowering of critical Reynolds numbers). This result can be appropriately used in the design of channel walls with appropriate velocity slip depending on the relevant applications. For all β values considered in this study, the Schmidt number (Sc) has a destabilizing effect on both the TS and the DD modes of instability. On the other hand, the ratio of the rate of diffusion (δ) has a stabilizing effect on the TS mode but destabilizing effect on the DD mode, for the above configuration.

The configuration with a higher viscous fluid adjacent to the slippery channel wall ($R_f + R_s > 0$) is unstable due to total viscosity stratification (similar to the SC system) and velocity slip at the wall destabilizes the DD system. The physical mechanism of stabilizing or destabilizing role of velocity slip at the walls of the channel on the DD-mode instability is explained through energy budget analysis. This theoretical investigation lends itself to verification by experiments and direct numerical simulations.

ACKNOWLEDGMENTS

The authors sincerely thank the referees for their very valuable suggestions and useful comments. These have improved the content and quality of the manuscript. The authors also thank the editor, Professor L. Gary Leal for his supporting remarks and suggestions. Our sincere thanks to Professor Rama Govindarajan for many useful and valuable suggestions and discussions.

APPENDIX A: JUSTIFICATION OF PARALLEL FLOW ASSUMPTION

In general, the concentration profiles of the slower and faster diffusing species should depend upon x. The parallel flow approximation is valid at large Reynolds and Péclet numbers, and we restrict ourselves to presenting results in this regime. It was discussed in Sahu and Govindarajan[18] that this mixed layer diffuses at a rate proportional to the inverse of Péclet number ($ReSc$). Thus, the downstream growth of the interface is very small at high Reynolds number. For Reynolds number of the order of 100, the parallel flow approximation is justified unless $Sc << 1$. As our Reynolds numbers considered are always greater than 100, we are in a safer side.

The present study is based on the parallel flow assumption in the mixed layer. This is equivalent to considering that the variations of the gradients in flow variables at the steady state and the thickness q of the mixed region have a much larger length scale than the disturbance wavelength.

The following discussion shows that the above assumption is justified for slow diffusion (higher values of Péclet number).

Let a splitter plate be located at $x < x_0$, at a constant y and let the parallel streams of two miscible fluids flow on both sides of this plate. The streams come into contact with each other at $x = x_0$. The two fluids begin to mix with each other for $x > x_0$, thus producing a stratified layer. The thickness 'q' of this layer grows as the fluids move downstream, and therefore q is a function of x. In what follows, it is shown that the thickness of the mixed layer varies slowly in x, i.e., $\partial q/\partial x << 1$.

We know at any location, the steady mean concentrations f and s corresponding to two spices F and S satisfy the equations

$$U\frac{\partial f}{\partial x} + V\frac{\partial f}{\partial y} = \frac{\delta}{Pe}\left[\frac{\partial^2 f}{\partial x^2} + \frac{\partial^2 f}{\partial y^2}\right], \tag{A1}$$

$$U\frac{\partial s}{\partial x} + V\frac{\partial s}{\partial y} = \frac{1}{Pe}\left[\frac{\partial^2 s}{\partial x^2} + \frac{\partial^2 s}{\partial y^2}\right], \tag{A2}$$

respectively. Now, under the boundary layer approximation ($V \ll U$ and $\frac{\partial^2}{\partial x^2} \ll \frac{\partial^2}{\partial y^2}$), we will get from Eq. (A1)

$$U\frac{\partial f}{\partial x} \simeq \frac{\delta}{Pe}\frac{\partial^2 f}{\partial y^2}. \tag{A3}$$

Also, using the same approximation, we know that $U \sim O(1)$, $y \sim \sqrt{\nu}$, where ν is the kinematic viscosity. Note that the viscosity is directly proportional to the concentration of each fluid in the mixed layer. Therefore, $qf \sim O(y^2)$ since f is the mean concentration over the mixed layer of thickness q. This implies that $\partial f/\partial x \simeq \frac{1}{q}O(\delta/Pe)$ (from Eq. (A3)). Similarly, from Eq. (A2), we can get $\partial s/\partial x \simeq \frac{1}{q}O(1/Pe)$. So, for large values of Pe, $\partial f/\partial x$, $\partial s/\partial x$ are very small showing that the downstream variation of f and s are very small which in turn implies that the changes in the thickness q of the mixed layer along the x-direction is very small.

Again, taking a similarity solution $f(y/q(x)) \simeq f(\xi)$ (where $\xi = (y/q(x))$) for Eq. (A3), we will get

$$U\frac{df}{d\xi}\left(-\frac{\xi}{q}\frac{dq}{dx}\right) \simeq \frac{\delta}{Pe}\left(\frac{d^2 f}{d\xi^2}\frac{1}{q^2}\right). \tag{A4}$$

As a consequence,

$$\frac{1}{q}\frac{dq}{dx} \sim \frac{\delta}{q^2 Pe} \Rightarrow \frac{dq}{dx} \sim \frac{1}{q}O\left(\frac{\delta}{Pe}\right). \tag{A5}$$

Thus, the downstream growth of mixed layer is inversely proportional to the Péclet number as U and ξ are of $O(1)$ and $O\left(\frac{ds}{d\xi}\right) \simeq O\left(\frac{d^2 s}{d\xi^2}\right)$, which confirms that for the Reynolds and Schmidt numbers considered in the present study, the assumption of uniform thickness of viscosity stratified layer (mixed layer) is justified.

APPENDIX B: DIFFERENT MIXED LAYER THICKNESS FOR FASTER AND SLOWER DIFFUSING SPECIES

The assumption of same mixed layer thickness q for the two species is valid only for $\delta \simeq 1$ where δ is the ratio of the rate of diffusions of the species. For $\delta \gg 1$, in reality, the mixed layer thickness of the faster diffusive species is expected to be larger than that of the slower diffusing species. In view of this, we have performed the computations with $q_f = \sqrt{\delta}q_s = 0.1$ (obtained from Appendix A) for $\delta = 6$ where q_f and q_s are the layer thicknesses corresponding to faster and slower diffusing species. The other parameters are $R_s = 2.0$, $R_f = -3.1$, $Sc = 30$, and $h = 0.6$. Fig. 14(a) shows the base velocity profiles for the cases $q_f = q_s = q = 0.1$ and $q_f = \sqrt{\delta}q_s = 0.1$ when $\delta = 6$, $\beta = 0.01$. Fig. 14(b) is the zoom of Fig. 14(a) near the mixed layer. Fig. 14(c) shows the

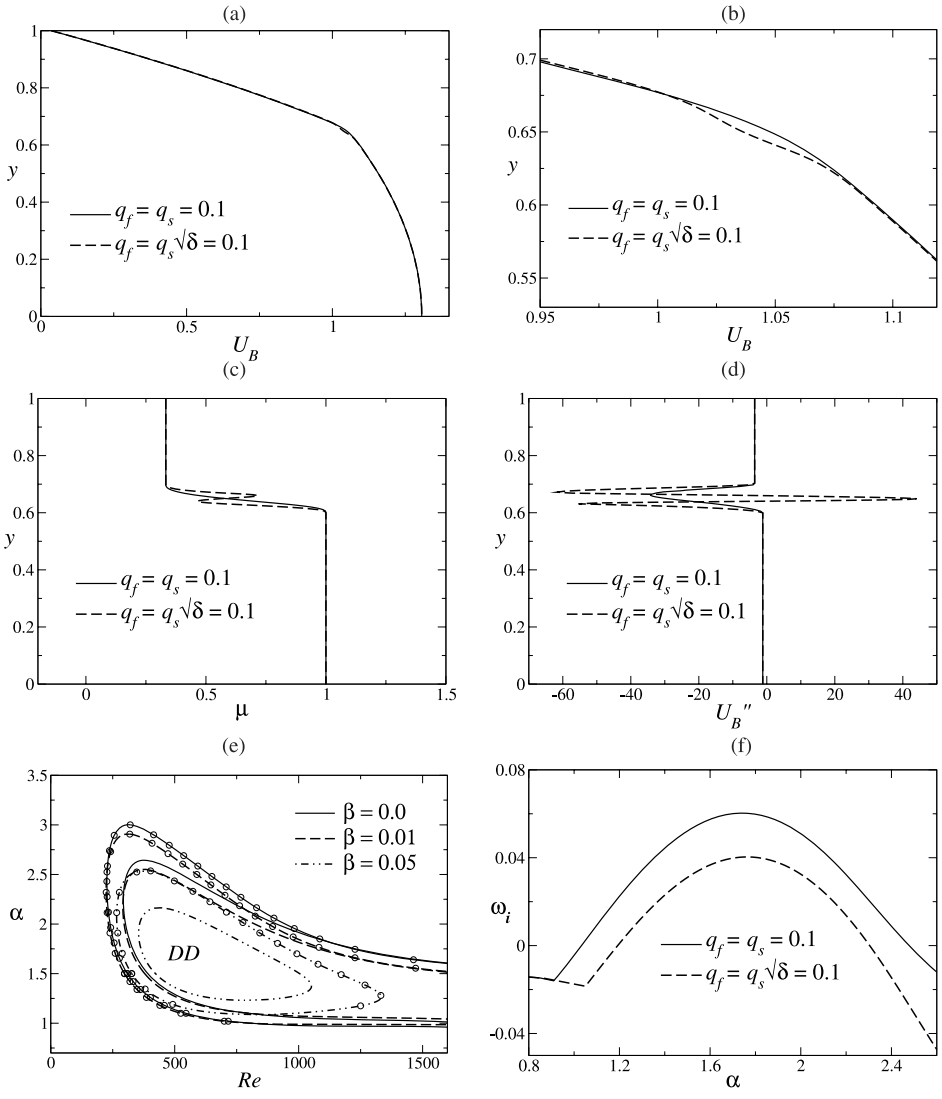

FIG. 14. (a) Base state velocity profiles for $\beta = 0.01$; (b) zoom of Fig. 14(a); (c) base state viscosity profiles for $\beta = 0.01$; (d) U_B'' as a function of y for $\beta = 0.01$; (e) neutral stability maps for $q_f = \sqrt{\delta} q_s = 0.1$ (without symbols) and $q_f = q_s = 0.1$ (with symbols); (f) growth rate (ω_i) versus wave number (α) for $Re = 600$, $\beta = 0.01$. The rest of the parameter values are $R_s = 2$, $R_f = -3.1$, $Sc = 30$, $\delta = 6$, and $h = 0.6$.

variation of base viscosity across the channel for $\delta = 6$ with $q_f = \sqrt{\delta} q_s = 0.1$ and $q_f = q_s = 0.1$. We observe that viscosity is a non-monotonic function of y within the mixed layer for $q_f \neq q_s$. As the log-mobility ratio R_f and R_s corresponding to the faster and slower diffusing species are of opposite signs, the variation in concentration is monotonically decreasing (monotonically increasing) for the faster (slower) diffusing species. Further, when $q_f \neq q_s$, $f_B(y)$ and $s_B(y)$ (given by Eqs. (16) and (17)) are different due to their dependence on q_f and q_s, respectively. Note that in the mixed layer, the base viscosity profile is $\mu_m(y) = \exp\left[R_s\, s_B(y) + R_f\, f_B(y)\right]$. As a result, the base viscosity profile for the case $q_f \neq q_s$ is non-monotonic in the mixed layer. Fig. 14(d) shows U_B'' as a function of y and we see that there is an inflectional point in the mixed layer for $q_f \neq q_s$. The neutral stability curves presented in Fig. 14(e) show that the above configuration (with $q_f \neq q_s$) is unstable for a wide range of wave numbers and that slip shrinks the unstable region as well as reduces the range of unstable wave numbers. However, the system with $q_f = q_s = q = 0.1$ is more unstable than the above case for each β considered. This may be attributed to the increase in base velocity in the

mixed region for the case $q_f = q_s = 0.1$ as compared to that for $q_f \neq q_s$ (Fig. 14(b)). Fig. 14(f) presents the growth rate curve corresponding to $q_f \neq q_s$ and $q_f = q_s$ for $Re = 600$ and $\beta = 0.01$.

We note from Figs. 14(c) and 14(d) that the base viscosity profile is monotonic, smooth (Fig. 14(c)) and the flow is inviscidly stable by Rayleigh's theorem[21] (Fig. 14(d); solid line with no point of inflection) for the case $q_f = q_s = q = 0.1$. As we want to examine the slip effects on the stability of the inviscidly stable "DD" system by taking mixed layer between two fluids having very small difference in viscosities so that the base viscosity variation within the mixed layer of small thickness is very smooth, continuous, and monotonic; in this study, the computations are performed by considering $q_f = q_s = q$.

[1] S. Ghosh, R. Usha, and K. C. Sahu, "Linear stability anlysis of miscble two-fluid flow in a channel with velocity slip at the walls," Phys. Fluids **26**, 014107 (2014).
[2] Y. Zhu and S. Granick, "Rate-dependent slip of Newtonian liquid at smooth surfaces," Phys. Rev. Lett. **87**, 096105 (2001).
[3] P. A. Thompson and S. M. Troian, "A general boundary condition for liquid flow at solid surfaces," Nature **389**, 360 (1997).
[4] J. W. Hoyt, "Hydrodynamic drag reduction due to fish slimes, swimming and flying," Nature **2**, 653 (1975).
[5] D. W. Bechert, M. Bruse, W. Hage, and R. Meyer, "Fluid mechanics of biological surfaces and their technological applications," Naturwissenschaften **87**, 157 (2000).
[6] E. H. Kennard, *Kinetic Theory of Gases* (McGraw-Hill, New York, 1938).
[7] G. A. Bird, *Molecular Gas Dynamics and the Direct Simulation of Gas Flows* (Oxford University Press, Great Clarendon Street, Oxford, 1994).
[8] M. M. Denn, "Extrusion instabilities and wall slip," Annu. Rev. Fluid Mech. **33**, 265 (2001).
[9] D. C. Tretheway and C. D. Meinhart, "Apparent fluid slip at hydrophobic microchannel walls," Phys. Fluids **14**, L9 (2002).
[10] J. Kim and C. J. Kim, "Nanostructured surfaces for dramatic reduction of flow resistance in droplet-based microfluidics," in *Technical Digest*, *IEEE Conference on MEMS, Lasvegas, NV* (2002), p. 479.
[11] R. Govindarajan, "Effect of miscibility on the linear instability of two-fluid channel flow," Int. J. Multiphase Flow **30**, 1177 (2004).
[12] X. Y. You and J. R. Zheng, "Stability of liquid-liquid stratified microchannel flow under the effects of boundary slip," Int. J. Chem. React. Eng. **7**, A85 (2009).
[13] M. Webber, "Instability of fluid flows, including boundary slip," Doctoral thesis, Durham University, 2007. Available at Durham E-Theses Online: http://etheses.dur.ac.uk/2308/.
[14] J. S. Turner, "Double-diffusive phenomena," Annu.Rev. Fluid Mech. **6**, 37–54 (1974).
[15] H. E. Huppert, "On the stability of a series of double-diffusive layers," Deep-Sea Res. Oceanogr. Abstr. **18**(10), 1005–1021 (1971).
[16] B. D. May and D. E. Kelley, "Effect of baroclinicity on double-diffusive interleaving," J. Phys. Oceanogr. **27**, 1997–2008 (1997).
[17] M. G. Worster, "Time-dependent fluxes across double-diffusive interfaces," J. Fluid Mech. **505**, 287-307 (2004).
[18] K. C. Sahu and R. Govindarajan, "Linear stability of double-diffusive two-fluid channel flow," J. Fluid Mech. **687**, 529 (2011).
[19] K. C. Sahu and R. Govindarajan, "Spatio-temporal linear stability of double-diffusive two-fluid channel flow," Phys. Fluids **24**, 054103 (2012).
[20] K. C. Sahu, "A review on double-diffusive instability in viscosity stratified flows," Proc. Natl. Acad. Sci., India **80**(3), 513–524 (2014).
[21] W. O. Criminale, T. L. Jackson, and R. D. Joslin, *Theory and Computation of Hydrodynamic Stability* (Cambridge University Press, New York, 2003).
[22] D. D. Joseph, R. Bai, K. P. Chen, and Y. Y. Renardy, "Core-annular flow," Annu. Rev. Fluid Mech. **29**, 65 (1997).
[23] D. Pritchard, "The linear stability of double-diffusive miscible rectilinear displacements in a Hele-Shaw cell," Eur. J. Mech., B: Fluids **28**(4), 564–577 (2009).
[24] Y. Nagatsu, K. Matsuda, Y. Kato, and Y. Tada, "Experimental study on miscible viscous fingering involving viscosity changes induced by variations in chemical species concentrations due to chemical reactions," J. Fluid Mech. **571**, 475–493 (2007).
[25] T. Podgorski, M. C. Sostarecz, S. Zorman, and A. Belmonte, "Fingering instabilities of a reactive micellar interface," Phys. Rev. E **76**, 016202 (2007).
[26] S. Swernath and S. Pushpavanam, "Viscous fingering in a horizontal flow through a porous medium induced by chemical reactions under isothermal and adiabatic conditions," J. Chem. Phys. **127**, 204701 (2007).
[27] P. Grosfils, F. Dubois, C. Yourassowsky, and A. De Wit, "Hot spots revealed by simultaneous experimental measurement of the two-dimensional concentration and temperature fields of an exothermic chemical front during finger-pattern formation," Phys. Rev. E **79**, 017301 (2009).
[28] H. Hejazi, P. Trevelyan, J. Azaiez, and A. De Wit, "Viscous fingering of a miscible reactive A+B=C interface: A linear stability analysis," J. Fluid Mech. **652**, 501–528 (2010).
[29] Q. Cao, A. L. Ventresca, K. R. Sreenivas, and A. K. Prasad, "Instability due to viscosity stratification downstream of a centerline injector," Can. J. Chem. Eng. **81**, 913 (2003).
[30] M. Regner, M. Henningsson, J. Wiklund, K. stergren, and C. Trgrdh, "Predicting the displacement of Yoghurt by water in a pipe using CFD," Chem. Eng. Technol. **30**, 844 (2007).
[31] R. Govindarajan and K. C. Sahu, "Instabilities in viscosity-stratified flows," Annu. Rev. Fluid Mech. **46**, 331–353 (2014).
[32] B. T. Ranganathan and R. Govindarajan, "Stabilisation and destabilisation of channel flow by location of viscosity-stratified fluid layer," Phys. Fluids **13**(1), 1 (2001).

[33] P. Ern, F. Charru, and P. Luchini, "Stability analysis of a shear flow with strongly stratified viscosity," J. Fluid Mech. **496**, 295 (2003).
[34] S. V. Malik and A. P. Hooper, "Linear stability and energy growth of viscosity stratified flow," Phys. Fluids **17**, 024101 (2005).
[35] E. J. Hinch, "A note on the mechanism of the instability at the interface between two shearing fluids," J. Fluid Mech. **144**, 463 (1984).
[36] M. J. South and A. P. Hooper, "Linear growth in two-fluid plane Poiseuille flow," J. Fluid Mech. **381**, 121 (1999).
[37] K. C. Sahu, A. Sameen, and R. Govindarajan, "The relative roles of divergence and velocity slip in the stability of plane channel flow," Eur. Phys. J.: Appl. Phys. **44**, 101 (2008).
[38] M. d'Olce, J. Martin, N. Rakotomalala, D. Salin, and L. Talon, "Pearl and mushroom instability patterns in two miscible fluids' core annular flows," Phys. Fluids **20**, 024104 (2008).
[39] M. Mishra, P. M. J. Trevelyan, C. Almarcha, and A. De Wit, "Influence of double diffusive effects on miscible viscous fingering," Phys. Rev. Lett. **105**, 204501 (2010).
[40] B. Selvam, S. Merk, R. Govindarajan, and E. Meiburg, "Stability of miscible core-annular flows with viscosity stratification," J. Fluid Mech. **592**, 23 (2007).
[41] K. C. Sahu, H. Ding, and O. K. Matar, "Numerical simulation of non-isothermal pressure-driven miscible channel flow with viscous heating," Chem. Eng. Sci. **65**, 3260–3267 (2010).
[42] M. Mishra, A. De Wit, and K. C. Sahu, "Double diffusive effects on pressure-driven miscible displacement flows in a channel," J. Fluid Mech. **712**, 579–597 (2012).
[43] G. I. Taylor, "Deposition of viscous fluid on the wall of a tube," J. Fluid Mech. **10**, 161 (1961).
[44] R. Balasubramaniam, N. Rashidnia, T. Maxworthy, and J. Kuang, "Instability of miscible interfaces in a cylindrical tube," Phys. Fluids **17**, 052103 (2005).
[45] H. H. Hu and D. D. Joseph, "Lubricated pipelining: Stability of core-annular flows. Part 2," J. Fluid Mech. **205**, 359 (1989).
[46] C. Kouris and J. Tsamopoulos, "Dynamics of axisymmetric core-annular flow in a straight tube. II. The less viscous fluid in the core, saw tooth waves," Phys. Fluids **14**, 1011 (2002).
[47] P. Huerre and P. A. Monkewitz, "Local and global instability in spatially developing flows," Annu. Rev. Fluid Mech. **22**, 473 (1990).
[48] K. C. Sahu, P. Valluri, H. Ding, and O. K. Matar, "Linear stability analysis and numerical simulation of miscible channel flow," Phys. Fluids **21**, 042104 (2009).
[49] J. P. Pascal, "Linear stability of fluid flow down a porous inclined plane," J. Phys. D: Appl. Phys **32**, 417 (1999).
[50] L. I. Mussel and R. Glang, *Handbook of Thin Film Technology* (McGraw-Hill, New York, 1970).
[51] P. Neogi and C. A. Miller, "Spreading kinetics of a drop on a rough solid surface," J. Colloid Interface Sci. **92**, 338 (1983).
[52] C. H. Choi, K. J. A. Westin, and K. S. Breur, "Apparent slip flows in hydrophilic and hydrophobic microchannels," Phys. Fluids **15**, 2897 (2003).
[53] Y. K. Watanabe and H. Mizunuma, "Slip of Newtonian fluids at solid boundary," JSME. Int. J., Ser. B **41**, 525 (1998).
[54] R. Pit, H. Hervet, and L. Leger, "Direct experimental evidence of slip in hexadecane: Solid interfaces," Phys. Rev. Lett. **85**, 980 (2000).
[55] E. Bonaccurso, M. Kappl, and H. J. Butt, "Hydrodynamic force measurements: Boundary slip of hydrophobic surfaces and electrokinetic effects," Phys. Rev. Lett. **88**, 076103 (2002).
[56] Y. X. Zhu and S. Granick, "Limits of hydrodynamic no-slip boundary condition," Phys. Rev. Lett. **88**, 106102 (2002).
[57] O. I. Vinogradova, "Slippage of water over hydrophobic surfaces," Int. J. Miner. Process. **56**, 31 (1999).
[58] J. M. Gersting, "Hydrodynamic stability of plane porous slip flow," Phys. Fluids **17**, 2126 (1974).
[59] A. Spille and H. B. A. Rauh, "Critical curves of plane Poiseuille flow with slip boundary conditions," Nonlinear Phenom. Complex Syst. **3**, 171 (2000).
[60] C. J. Gan and Z. N. Wu, "Short-wave instability due to wall slip and numerical observation of wall-slip instability for microchannel flws," J. Fluid Mech. **550**, 289 (2006).
[61] E. Lauga and C. Cossu, "A note on the stability of slip channel flows," Phys. Fluids **17**, 088106 (2005).
[62] R. Ling, C. Jian-Guo, and Z. Ke-Qin, "Dual role of wall slip on linear stability of plane Poiseuille flow," Chin. Phys. Lett. **25**, 601 (2008).
[63] L. Ren and D. H. Xia, "Generalized Reynolds-Orr Energy Equation with Wall Slip," Appl. Mech. Mater. **117-119**, 674–678 (2011).
[64] A. Beskok and G. E. Karniadkis, *Micro Flows Fundamentals and Simulation* (Springer, London, 2002).
[65] D. P. Wall and S. K. Wilson, "The linear stability of channel flow of fluid with temperature dependent viscosity," J. Fluid Mech. **323**, 107 (1996).
[66] T. Min and J. Kim, "Effects of hydrophobic surface on stability and transition," Phys. Fluids **17**, 108106 (2005).
[67] E. Lauga, M. P. Brenner, and H. A. Stone, in *Hand book of Experimental Fluid Dynamics*, edited by J. F. Foss, C. Tropea, and A. Yarin (Springer, NewYork, 2005).
[68] P. G. Drazin and W. H. Reid, *Hydrodynamic Stability* (Cambridge University Press, Cambridge, 1985).
[69] C. Canuto, M. Y. Hussaini, A. Quarteroni, and T. A. Zang, *Spectral Methods in Fluid Dynamics* 1st ed. (Springer Verlag, New York, 1987).